APPLICATION OF SIMPLE SMART LOGIC FOR WATERFLOODING RESERVOIR MANAGEMENT

A Thesis

by

MARCELO JACQUES DALL'AQUA

Submitted to the Office of Graduate and Professional Studies of
Texas A&M University
in partial fulfillment of the requirements for the degree of

MASTER OF SCIENCE

Chair of Committee,	Eduardo Gildin
Committee Members,	John E. Killough
	Maria A. Barrufet
Head of Department,	A. Daniel Hill

December 2016

Major Subject: Petroleum Engineering

ABSTRACT

A simple smart logic for controlling inflow control valves (ICV) in waterflooding reservoir management is implemented and analyzed, with the final objective of improving the long term financial return of a petroleum reservoir.

Such a control is based in a reactive simple logic that responds to the watercut measured in the ICV. Basically, when the watercut increases, the ICV is set to close proportionally. For comparison purposes, four strategies are presented: base case scenario with conventional control, the best completion configuration found by trial-and-error, the reactive control, and a deterministic optimal control based on Nonlinear Gradient Method with adjoint-gradient formulation is shown for comparison purposes. Finally, all four strategies are tested again in different reservoir realizations in order to mimic the geological uncertainties.

Two different synthetic reservoir models were studied. First, a simple cube with a five-spot well configuration, in which the permeability field has a horizontal pattern defined by lognormal distributions. The second model is a benchmark proposed by the Dutch university, TU delft, with 101 channelized permeability fields representing river patterns.

For the first model, no significant relative gain is found neither in the variable control nor in the optimal control. Manly because of the high homogeneity of the reservoir models. Therefore, no intelligent completion is recommended. On the other hand, for the second and more complex case, the results indicate an expressive relative gain in the use of simple reactive logic. Besides, this type of control achieves results nearly as good as the optimal control.

The test in different realizations, however, shows that reservoir characterization is

still a key part of any attempt to improve production. Although the variable reactive control is semi-independent, with action being taken based on measurements, some parameters need a priori model to be tuned.

ACKNOWLEDGMENTS

First of all, I would like to express my sincere gratitude to my advisor Dr. Eduardo Gildin for all advices, continuous support, patience, comprehension, encouragement and knowledge he gave me during these two years in my master degree. His motivation was very important to finish this journey. Without his guidance nothing would be possible.

Furthermore, I would like to thank Dr. Killough and Dr. Barrufet for being part of my graduate committee. I would like to thank them for their time, kind relation and insightful questions they asked me.

I thank my fellow colleagues for their friendship, stimulating discussions, for the sleepless nights we were working together, and for all the fun we had together.

Also, I would like to thank my mother Maria do Carmo and my father Renato for all motivation, stimulation and positive thinking they gave me not only these two years I spend as an Aggie, but during all my life. Regarding my young brother, Fernando, we both took a master in USA at the same time, but in different Universities. Our phone calls were very important to share our frustrations and also our achievements during all the time.

And finally, I would like to thank the most important person in my life, my wife Fabiane. I do not have words enough to thank her for all she has been doing for me. Her love, motivation, comprehension, patience, encouragement and hugs were very important to me day by day. She was present in every moment of this journey, either giving me support in the sad moments, or celebrating our victories, or even scolding me when I was lazy. Without her precious support nothing would be possible. Moreover, I can even say that this thesis is her accomplishment too.

CONTRIBUTORS AND FUNDING SOURCES

This work was supervised by a thesis committee consisting of Professor Dr. Eduardo Gildin and Dr. John Killough of the Department of Petroleum Engineering and Professor Dr. Maria Baruffet of the Department of Chemical Engineering.

All work for the thesis (or) dissertation was completed by the student, under the advisement of Dr. Eduardo Gildin of the Department of Petroleum Engineering.

Funding Sources

Graduate study was supported by a scholarship from the CAPES Foundation, Ministry of Education of Brazil, Brasilia – DF, Zip Code 70.040-020 - under the "Brazil Scientific Mobility Program" program.

TABLE OF CONTENTS

Page

LIST OF FIGURES

FIGURE Page

LIST OF TABLES

TABLE Page

1. INTRODUCTION

The alleged rising global demand for energy combined with a relative lower oil price scenario is creating a difficult climate to oil producers companies. Especially after the events in 2014 (when oil prices fell dramatically causing the biggest crisis in the sector since 1986), companies are pushed to be more efficient (i.e doing the things right) and effective (i.e. doing right things) to thrive.

Because development and discovery of new fields are very expense, risky and very long term return, increasing efforts to better develop mature fields has been increased in last decades (Babadagli 2007). So, the hypothesis of this research is that we can improve recovery utilizing the conventional methods of water flood together with automated control schemes when compared with traditional reactive action taken place on a daily production basis.

Regarding reservoir engineers, the challenge looks pretty simple: produce more oil from the reservoir in an economic way. Nevertheless, fossil-fuel producers face multiple uncertainties coming from all directions: economics, geopolitics, geology, technology and policy. These aspects make the reservoir optimization a very challenging task, and maybe impossible. Therefore, other goal is to apply a simpler approach that reach a practical near-optimal result (i.e. not perfect but good).

1.1 Economic Environment

In the last two years, the oil market has suffered the most turmoil since 1986. Oil price has fallen from a relatively stable and high level of approximately USD 100 dollars in the period of 2010 to mid-2014 to USD 30-40 dollars by March 2015. That being said, this section has the objective of making a deep economic analyses in energy business.

Such a debacle not only was unforeseen, but also underestimated: fig. 1.1 shows the predictions by the U.S. Energy Information Administration (EIA 2014).

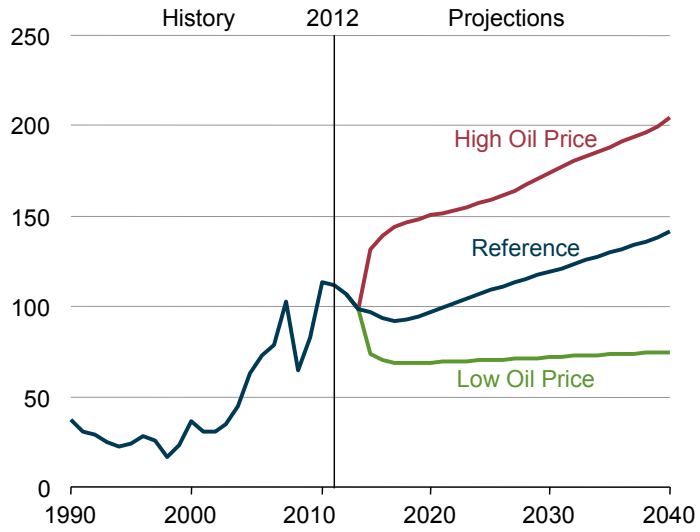

Figure 1.1: North Sea Brent crude oil spot prices in three case, 1990-2040 (reprinted with permission from EIA 2014)

This can be explained by the very complex forces that drive crude oil price. Out of the 7 factors that can influence the oil price cited by EIA (2016), the most correlated one is geopolitical events. Figure 1.2, for instance, shows the crude oil price from 1970 to 2015, in which sharp changes can be seen in some years: 1973 (Yom Kipur war), 1979 (Iran Revolution), 1986 (Saudi Arabia policy change), 2008 (Global financial crisis), and finally the most recent one in 2014. Such events are extremely difficult to foresee, because they depend on policy makers' decision and not on the classic analysis of supply versus demand (at least directly).

The most recent crash in 2014 can be explained by three factors: (1) slowdown in demand growth, (2) record increases in supply, particularity tight oil from North

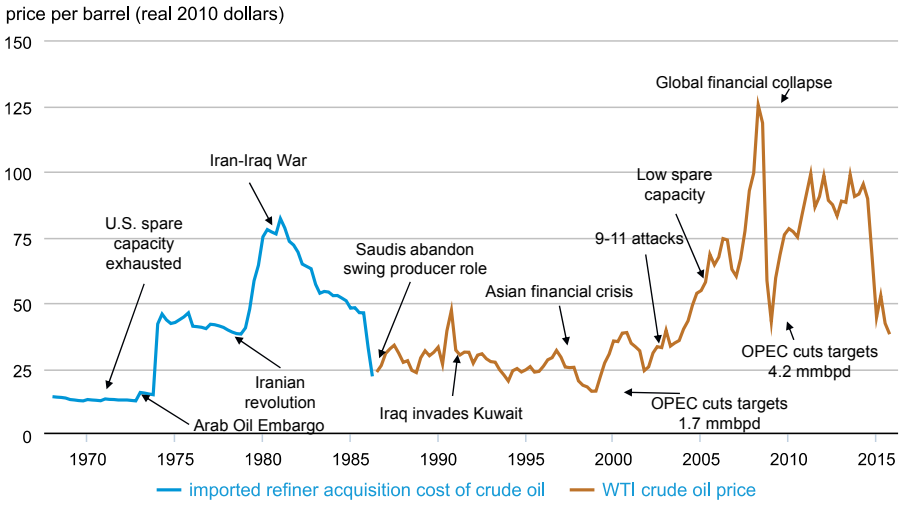

Figure 1.2: Crude oil prices react to a variety of geopolitical and economic events (reprinted with permission from EIA 2016)

America, and (3) a decision by the Organization of Petroleum Exporting Countries (OPEC) countries not to try to rebalance the market through cuts in output (IEA 2015). The latter had probably the most drastic effect, as the OPEC delegates reached a conclusion to shift its policy to keep the market share instead of protect the oil price. Doing this, they put the pressure of balancing the market on the non-OPEC countries, with the oil price as the mediator.

1.1.1 1986 vs 2014

It is import to make comparison between oil price decreases in 1986 and 2014; understanding its similarities and differences and then predicting the market response can allow companies to manage its budgets for the next years. For instance, the implications of the first fall lasted until the 2000s when China boosted the demand. Some similarities with the 1986 fall are a preceded period with historically high prices that stimulated majors investments in non-OPEC countries (e.g. Noth Sea and Alaska in 1986; tight oil and tar sand in North America in 2014) and discouraged

global demand, and the decision of the OPEC countries to preserve market share. Yet there are important differences as well: the OPEC countries had a huge spare capacity in the 80s. Due to its previous policy of price control they deliberated decreased their market share from 50% in the 70s to 30% in '85 (Saudi Arabia crude output fell from 10 md/d in 1980 to 3.4 mb/d in 1985). Today there is no such analogy, spare capacity is relatively limited by historical standards as of mid-2015. Regarding the non-OPEC side, the US tight oil, which has been proved to be extremely resilient, is a source of supply more responsive to market price fluctuations and smaller in terms of recoverable resources (IEA 2015).

The duration of this low price scenario seems to remain ultimately in the hands of OPEC countries. Their strategy of market share is likely to succeeded given its enormous and cheap reserves compared to the rest of the world. However, such a strategy comes with some drawbacks as well; the fiscal finance of some members is quickly deteriorating with the losses from lower oil prices being bigger than the gain from higher volumes over the long term (The Economist 2016; Rascouet 2015; Hirst 2014). Because of this, according to IEA 2015, a long period of low oil prices is unlikely to happen, and eventually the oil price will go up, and the main question of "when?" will depend on the resilience players.

1.1.2 Demand

Predictions of demand and, specifically, oil price are notable for their failures (see fig. 1.1). To asses this issue, the IEA (2015) put forth a study including four scenarios which differ in their assumptions about the evolution of energy-related government policies with the base year for all of the scenarios being 2013:

- New Policies Scenario: "In addition to incorporating the policies and measures that affect energy markets and that had been adopted as of mid-2015, it also

takes account of other relevant intentions that have been announced, even when the precise implementing measures have yet to be fully defined".

- Current Policies Scenario: It "takes into consideration only those policies for which implementing measures had been formally adopted as of mid-2015 and makes the assumption that these policies persist unchanged".

- 450 Scenario: It "assumes a set of policies that bring about a trajectory of greenhouse-gas (GHG) emissions from the energy sector that is consistent with the goal to limit the rise in the long-term average global temperature to two degrees Celsius (2℃)".

- Low Oil Price Scenario: It "illustrates the impact of a persistently lower oil price than that modeled in the New Policies Scenario. In this scenario, market equilibrium is not attained until the 2020s, with prices in the USD 50-60/barrel range (in year 2014 dollars), after which the price starts to edge higher, reaching USD 85/barrel in 2040".

The results can be seen in fig. 1.3. Oil price rises in all scenarios, including "Low price scenario", at a lower pace though. Oil demand increases too with exception of the "450 Scenario". From all 4 scenarios, the most likely to happen according IEA 2015 is the "New Policies Scenario" in the medium term. The plausibility of "Low Oil Price Scenario" will depend on the strength of some factors: "World lower near-term gross domestic product (GDP), the return of Iran to the international oil market, a robust outlook for tight oil in the United States" and fiscal finance of the OPEC members. As time passes those forces tend to weaken making this scenario less probable. "Current Policies Scenario" by definition is clearly extremely unlikely to be realized, but it offers a benchmark of how global energy markets would evolve

without new policy intervention. "450 Scenario" would require a much stronger World commitment to address climate change, that involves a deeper industry shift to less carbon depended sources of energy and all the inherent infrastructure cost (Jones et al. 2016).

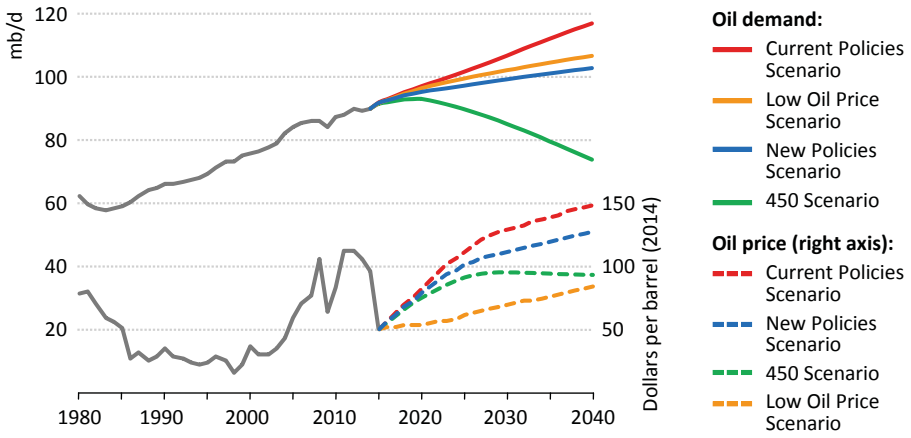

Figure 1.3: World oil demand and price by scenario (reprinted with permission from IEA 2015)

Sectoral trends

A deeper analysis of the demand should pay attention to the sectoral trends. A detailed focus is based in the "New policies scenario", the most likely to happen as explained in section 1.1.2. The table 1.1 leads to some important conclusions: demand for oil likewise remains strong in the transport sector and as a feedstock for the production of petrochemicals. For the former, the only thing that can threaten the oil domain is the electric cars, but their success depends on improvements in more efficient and cheaper batteries, as well as consumers' preferences regarding some limitations like driving range, recharging times and availability of recharging

stations. In the petrochemical sector, on the other hand, there are currently no competitiors to napha and ethane (products from oil). Outside these domains, oil has long been in retreat.

In addition, according to table 1.1, one can reach the conclusion that renewable energies do not compete directly with crude oil. Those kind of sources (hydro, wind and solar) play an important role in the power generation sector, thus competing directly with natural gas and coal.

Table 1.1: World oil demand by sector in the New Policies Scenario (mb/d)(reprinted with permission from IEA 2015)

	2000	2014	2020	2025	2030	2035	2040	2014-2040	
								Change	CAAGR*
Power generation	5.8	5.3	4.4	3.7	3.2	3.0	2.8	-2.5	-2.4%
Transport	38.8	49.5	53.2	55.4	57.3	58.9	60.4	10.9	0.8%
Petrochemicals	9.5	11.5	14.1	14.9	15.8	16.6	17.2	5.6	1.5%
Feedstocks	8.1	10.1	12.5	13.3	14.1	14.9	15.5	5.4	1.7%
Other industry	4.9	4.9	5.1	5.1	5.1	5.1	5.2	0.3	0.2%
Buildings	7.9	7.6	7.2	6.6	6.2	5.9	5.8	-1.8	-1.1%
Other**	9.9	11.7	11.9	12.1	12.2	12.3	12.2	0.5	0.2%
Total	**76.9**	**90.6**	**95.9**	**97.9**	**99.9**	**101.7**	**103.5**	**12.9**	**0.5%**

* Compound average annual growth rate. ** Other includes agriculture, transformation and other non-energy use (mainly bitumen and lubricants).

1.1.3 Supply

Different from other industries like electronics, the oil sector is highly dependent on nature (i.e. one cannot choose where the oil is). Therefore, before starting to analyze how to meet the demand, it is imperative to estimate location and type of resources. Table 1.2 gives some insights: despite the ascension of tight oil, crude oil remains the most important source, with Middle East in a privileged position having approximate 42% of all resources; regarding Unconventional resources, extra-heavy

oil and bitumen (EHOB) and kerogen oil have the greatest potential to improvements, but its high production cost can limit exploration.

Table 1.2: Remaining technically recoverable oil resources by type and region, end-2014 (billion barrels)(reprinted with permission from IEA 2015)

	Conventional resources		Unconventional resources			Total	
	Crude oil	NGLs	EHOB	Kerogen oil	Tight oil	Resources	Proven reserves
OECD	**320**	**150**	**809**	**1 016**	**118**	**2 414**	**250**
Americas	250	107	806	1 000	83	2 246	233
Europe	60	25	3	4	17	110	12
Asia Oceania	10	18	-	12	18	58	4
Non-OECD	**1 908**	**409**	**1 068**	**57**	**230**	**3 672**	**1 456**
E. Europe/Eurasia	265	65	552	20	78	980	146
Asia	127	51	3	4	56	242	45
Middle East	951	155	14	30	0	1 150	811
Africa	320	87	2	-	38	447	130
Latin America	244	50	497	3	57	852	325
World	**2 228**	**559**	**1 878**	**1 073**	**347**	**6 085**	**1 706**

Notes: Proven reserves (which are typically not broken down between conventional/unconventional) are usually defined as discovered volumes having at least 90% probability that they can be extracted profitably. EHOB is extra-heavy oil and bitumen. The IEA databases include NGLs from unconventional reservoirs (i.e. associated with shale gas) outside the United States, assuming similar gas wetness to that seen in the United States, because of the lack of comprehensive assessment; these unconventional NGLs resources are included in conventional NGLs for simplicity.

Sources: IEA databases; BGR (2014); BP (2015); OGJ (2014); US DOE/EIA/ARI (2013); USGS (2012a, 2012b).

Resources, however, are different from Reserves. The latter concept is related to economics (i.e, how much oil is economically producible, what is highly depend on oil price). Table 1.3 from IEA 2015 shows a prognostic of oil supply by type considering the aforementioned New Police Scenario. Although it is notable a decrease of importance along the years, crude oil remains the largest single output with 66% of total oil production by 2040 (compared to 87% in 2000 and 76% in 2014).

It is most important to realize the decline of existing fields, from 66.6 mb/d in 2014 to 23.8 mb/d in 2040, a 65% deterioration. Thus, a major effort must be done

Table 1.3: World oil supply by type in the New Policies Scenario (mb/d)(reprinted with permission from IEA 2015)

	2000	2014	2020	2025	2030	2035	2040	2014-2040	
								Change	CAAGR*
Conventional production	**73.8**	**81.9**	**82.6**	**84.5**	**85.1**	**85.6**	**85.9**	**4.0**	**0.2%**
Crude oil	65.5	68.0	67.3	68.4	67.9	67.4	66.8	-1.2	-0.1%
Existing fields	64.0	66.6	53.6	44.8	36.9	29.7	23.8	-42.7	-3.9%
Yet-to-be developed	-	-	12.4	17.7	19.3	20.8	22.3	22.3	n.a.
Yet-to-be found	-	-	-	3.7	8.7	13.1	16.3	16.3	n.a.
Enhanced oil recovery	1.4	1.4	1.4	2.2	3.1	3.8	4.4	2.9	4.4%
Natural gas liquids	8.3	13.9	15.2	16.1	17.2	18.2	19.2	5.2	1.2%
Unconventional production	**1.2**	**7.6**	**10.9**	**10.8**	**12.1**	**13.2**	**14.5**	**6.9**	**2.5%**
Tight oil	-	4.0	5.8	5.2	5.5	5.4	5.0	1.0	0.8%
Extra-heavy oil and bitumen	0.8	2.6	4.1	4.3	4.9	5.7	6.9	4.3	3.8%
Total production	**75.0**	**89.5**	**93.5**	**95.3**	**97.2**	**98.8**	**100.4**	**10.9**	**0.4%**
Processing gains	**1.8**	**2.2**	**2.4**	**2.6**	**2.7**	**2.9**	**3.0**	**0.8**	**1.2%**
Supply**	**76.9**	**91.7**	**95.9**	**97.9**	**99.9**	**101.7**	**103.5**	**11.8**	**0.5%**

* Compound average annual growth rate. ** Differences between historical supply and demand volumes shown earlier in the chapter are due to changes in stocks.

just to keep production flat and to compensate for declines in existing fields, rather than actually to meet the increase in demand. By the end of the projection period, 39 mb/d out of 66.8 mb/d will come from conventional oil fields that are either waiting to be developed or waiting to be discovered.

In this projection, the expected contribution of Enhanced Oil Recovery (EOR) plays a marginal but still important role, increasing its contribution from 1.4 mb/d in 2014 to 4.4 mb/d. EOR techniques encompass a range of sophisticated techniques to recover more oil than would be possible by utilizing only primary production or waterflooding (e.g. chemical flooding, miscible displacement and thermal recovery). It was not evaluated; however, possible gains can come from a better design of conventional recover method of waterflooding, which is the main focus of this thesis.

Investments

The required cumulative investments in the oil and gas sector are approximated to be USD 25 trillion in the "New Policies Scenario", of which 80% (USD 20 trillion) is in the upstream; finally, 85% (USD 17 trillion) of upstream investment is to keep today's levels of production (i.e. to compensate for decline of existing wells) (IEA 2015). This represents an annual average of USD 650 billion for keeping the crude oil production flat.

1.1.4 Final Remarks

In conclusion, World demand for crude oil is most likely to rise in the next decades, specially pushed by transport and petrochemicals sector. International oil companies (IOC) and national oil companies (NOC) will have to spend approximately USD 750 billion per year until 2040 in the upstream to meet this demand, of which USD 650 billion will be used to compensate natural decline of existing wells.

However, better oil recovery of mature fields can significantly decreased the amount of necessary money to compensate the decline production, since its investment is considerably less than greenfield projects.

1.2 Research Objective

The objective of this thesis is to implement and analyze smart logics with simple methodologies to improve the economical return of hydrocarbons reservoir in the long-term term production. In order to test the hypotheses of simple controllers, we will apply the simple logic in "intelligent wells" equipped with inflow-control valves on a project with the wells locations already defined.

1.3 Thesis Organization

Besides this introductory section, this thesis is organized in more five chapter. The second chapter gives a brief literature review on papers that works on reservoir optimization. The chapters three and four introduce the most relevant theoretical fundamentals, where chapter 3 mathematically explain the black oil model simulator and chapter 4 gives a brief overview on the optimization theory. Then, chapter five describes the methodology utilized in order to compare different scenarios. Finally, in chapter six, two different case were studied.

2. LITERATURE REVIEW

2.1 Basic Background

Oil recovery has been classified as primary, secondary and tertiary. Historically, but not always, these three phases happen in a chronological manner, so their names (thought somewhat outdated terminology). Primary production takes advantage of the initial high pressure of reservoir (i.e. energy) to make the fluid flow to surface. The main mechanism drives at this stage are: solution-gas and fluid expansion drive, gas-cap drive, waterdrive (e.g. underlying aquifer), gravity drive, and combination drive (Towler 2002). Regarding production, primary methods have a limited oil recovery range (table 2.1). Secondary methods consists of injecting immiscible fluid to maintain or recuperate reservoir fluid. Tertiary, which typically initiate after the secondary method exhausts, utilizes Enhanced Oil Recovery (EOR) methods such as injections of miscible gas, of polymers dissolved in water, or of chemicals.

Table 2.1: Driving mechanism oil recovery range (reprinted with permission from Ahmed 2010)

Driving Mechanism	Approximate Oil Recovery Range,%
Rock and liquid expansion	3-7
Solution gap	5-30
Gas cap	20-40
Water drive	35-75
Gravity drainage	<80
Combination drive	30-60

Waterflooding has been extensively used with effective and positive gains as the prime secondary method. Warner Jr. (2015) attributes its success to:

- Water injection provides pressure support to aid and enhance oil production;
- The water displacement of oil is a reasonably efficient process to recovery;
- In most situations around the world, there is a plentiful supply of water readily available, typically subsurface brines or offshore seawater;
- Water is the least-costly of the available fluids used for injection, and brines generally have no alternative use, unlike natural gas;
- In many situations, the water-oil-viscosity ratio is not too unfavorable so that the displacement process is relatively effective, compared to the has-oil-viscosity ratio.
- Water is reasonably easy to inject and requires little compression to achieve the desired injection pressure because of its high density and low compressibility, again compared to natural gas, which is low-density fluid at surface conditions and has high compressibility;
- water and oil are fairly easy to separate because they are immiscible with other, unless stable water-oil emulsions forms. Then, heat an or chemicals must be added to aid breaking the emulsions.

2.2 Conventional Waterflooding

Waterflood projects are design by the concept of "voidage replacement" (i.e. sufficient water must be inject to replace the volumes of produce fluids). The purpose is, then, pressure maintenance and displacement of oil from the pore space (sweep). Practically, in order to compensate fluid losses to underlying aquifers and adjacent formations, water injection is specified to be 5 to 10 % more than the sum of reservoir volumes of various producers fluids. In addition, the injections rates must be high

enough so that several hydrocarbon pore volumes (HCPVs) are injected during the project life, as a "rule of thumb" 10 to 15% of HCPVs per year (Warner Jr. 2015).

The duration of a project usually is 20 years or more. During this time, the water cut is monitored per producer well, since this value reach a non-economic feasible level the well is then shut-in. This economic threshold is determined case by case and takes into consideration several factors, such as: prices of oil and water treatment, facilities capacity to separate oil form water, etc.

2.3 Reservoir Management

The Reservoir Management concept has been in the industry for many years. Basically, it can be defined as the set of actions and decisions a reservoir suffer throughout its life from discovery to depletion and final abandonment. It depends on a integrated approach of human knowledge (from engineers, geoscientists, manager, etc) and technological resources in a constant loop cycle (data, analysis, action, monitoring) to obtain the maximum possible economic recovery (Wiggins et al. 1990; Satter et al. 1994; Thakur 1996).

In the last 15 years, due to advances on automation, academics have emphasized a more modern concept of "Real Time Reservoir Management"[1] (RTRM) or "Closed-Loop Reservoir Management" (CLRM). The idea is to have a near-continuous control of the reservoir instead of batch control, or in other words, to reduce considerably the time between data acquisition and action, what would significantly increase life-cycle value (Jansen et al. 2009). Hou et al. (2015) defined this concept, specifically to a waterflooding projects, as a technique that "enables a dynamic and real-time optimal production schedule under the existing reservoir conditions to be achieved

1. The term "real time" refers to making decisions at a frequency commensurate with the time-scale of the system. In the specific case of reservoir engineering, the slow dynamics allow low frequencies.

by adjusting the injection and production strategies".

The oil field is viewed, then, as a dynamic system (fig. 2.1) with many "states", (e.g. input and output variables). The inputs are those components in the reservoir that stimulates and control production such as flow choke settings, water injection rate, separator pressure, and artificial lift quantity. The outputs are the system's responses, they can be dived two sub group: measured variables, such as multiphase fluid rates and well flowing pressure; and unmeasured variables that can be estimated by a simulator, such as reservoir pressure and fluid saturations. In addition to states there are also the "parameters" of the system such as reservoir heterogeneity, fluids distribution, permeabilities, porosities and fault transmissibilities (Saputelli et al. 2005).

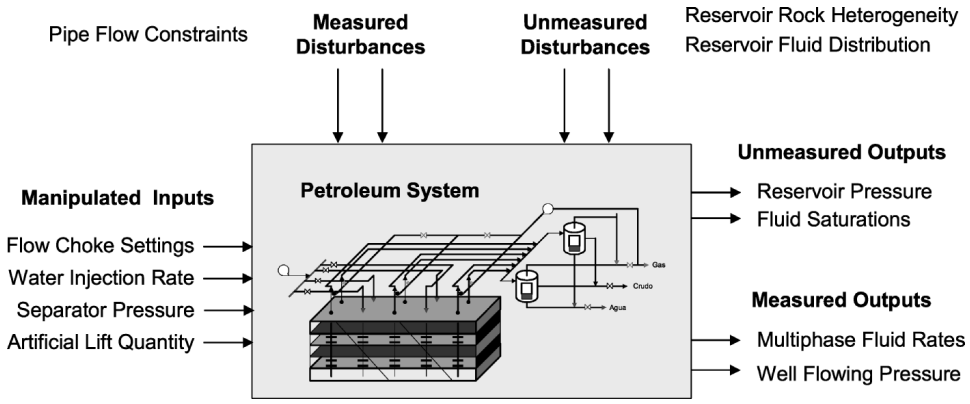

Figure 2.1: Petroleum system represented as a dynamic system (reprinted from Saputelli et al. 2005)

A key aspect of RTRM and also one of the biggest challenges to overcome is data assimilation. This term used in a broad sense refers to estimation of both states and parameter using measured output data. In a more restrict sense, consid-

ering only parameters, it is known in Petroleum industry as "History Matching", a jargon to inverse problem (because forward problems use a set of reservoir model variables to predict reservoir performance). The major issue of this technique is that almost always there are many possible combinations of parameters that result in same reservoir behaviors. This happens because the mathematical formulation is ill-posed. Moreover, reservoir heterogeneities are extremely difficult to characterize and usually are dealt by creative "insights" from geologists.

A different term, "Closed-loop Reservoir Management" (Jansen et al. 2009), is very common in the literature to refer to RTRM which reflects the fact that the system is closed by two loops: optimization and model updating. Figure 2.2 depicts this characteristic, in which the top represents the real reservoir, wells and facilities. The center represent the mathematical model (i.e. a reservoir simulator), which is derived by upscaling techniques of high-order model generated by geologist, seismics, well logs, etc. The blue loop correspond to control actions that impact in production (e.g. wellhead choke settings, injection rates, or more abstractly as decisions in a field development plan, such as the choice of well positions), such decisions depend on the state variables (i.e. pressures and saturations in the reservoirs, pressures and phase rates in the wells). The red loop correspond data assimilation process, which tries to reconcile the outputs (e.g. multiphase fluid rates and well flowing pressure) from both measured in the real reservoir and predicted by the simulator.

2.3.1 Model Based - Nonlinear Model Predictive Control

In order to overcome these limitations of pure Optimal Control (e.g. the lack of feedback information and assumption of previous knowledge of the reservoir), some early studies have tried to systematic implement both optimization and data assimilation simultaneously. For instance, Nævdal et al. (2006) used the Optimal Con-

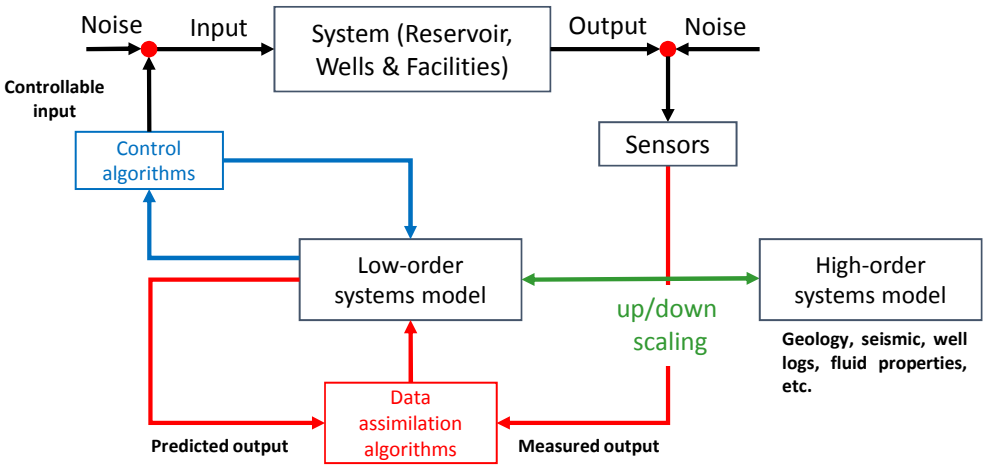

Figure 2.2: Layout of closed-loop reservoir management (adapted from Jansen et al. 2009)

trol Theory with adjoint formulation for production optimization and the ensemble Kalman filter (Evensen 2009) to sequentially perform state estimation. Similarly, Sarma et al. (2006) also used the same method for production optimization, but a Baysesian inversion theory in combination with an optimal representation of the unknowns parameter field in terms of Karhunen-Loeve expansion for history matching. Both papers approach the optimization issue by the adjoint formulation, a very computationally efficient method that, irrespective the number of variables, requires only one forward and one adjoint simulation to compute the gradient; the drawbacks, however, are that it takes a major programming effort and it requires access to the simulator code to compute the Jacobian, what is not possible in the commercial simulator (Jansen 2011).

Jansen et al. (2008) defined these attempts as a form of nonlinear model predictive control (NMPC) with a gradually "shrinking horizon". There is; however, a crucial difference from the classical NMPC used in the process industry: instead of aimed

to follow a predefined optimal trajectory, the NMPC in reservoir management is aimed to find that optimal trajectory to begin with (Jansen et al. 2008). Foss et al. (2011) also advocated for NMPC "because it balances closed-loop and open-loop in a way that is suitable for reservoir management", in other words, because of the very slow dynamics of the reservoir physics, it is possible to perform a computational optimization off-line (i.e. a simulation that takes a few days) and then change the controllable inputs (e.g water injection rates), all this in a periodically fashion.

2.3.2 Practical Issues

Nevertheless, closed loop reservoir management had repeatedly come under strong criticism and it has not been yet implemented entirely on the real project. The main issues are (1) the lack of robustness to deal with reservoir uncertainties, (2) impractical water rates injection suggested and conflict between short and long-term objectives.

Geological uncertainties

As explained before, history matching is a ill-posed problem, which means that completely different models can produce same results. No matter which technique used, the chances of a model to fully represent all the dynamics characteristic of a real reservoir are extremely low. Therefore, it seems pointless to perform a optimization to plan ten years of production in such models.

One way to deal with such problem is the so-called Robust Optimization (RO), that is, to use multiple subsurface models (i.e geological realizations) expecting that such realizations would reflect the range of all possible geological structures. Van Essen et al. (2009) applied such strategy creating 100 realizations of a 3D synthetical reservoir. They chose then the control strategy that maximized the expected net present value of all realizations, hoping with that to reduce, at least indirectly, the

risk.

On the other hand, Capolei et al. (2015) proposed the Sharpe Ratio (e.g. ratio between the expected mean NPV and the standard deviation of the mean) as the determining indicator instead of just expected NPV, dealing thus directly with the trade-off risk-return. The sharpe ratio, however, can be inaccurate when applied to portfolios or assets that do not have a normal distribution of expected returns (Investopedia 2011), which is the case of reservoir simulators.

However, although such strategy of Robust Optimization undoubtedly decreases the risk due uncertainties, it turns out to be very conservative and very time consuming (because the number of simulation is proportional of the number of realizations). Besides, real reservoirs are large scale system with approximate 10^6 grid cells, so there is no guarantee that those 100 realizations depict accurately the reservoir.

2.3.3 Practical Approach

Other issue is that model-based optimization (e.g optimization from a mathematical model) normally prescribes irregular settings, that is, controls commands like injection water rates that are too variable in time to make them implementable in real reservoirs. Such problem arises from a too mathematical approach that attempts to optimize a single objective (e.g NPV), ignoring practical limitations. For instance, production engineers have a very practical mindset, so is questionable if they would allow such strategies that are not at the maximum potential, specially because they are aware of the risks of uncertainties both in the reservoir parameters and in the oil price.

Very often there is a conflict between long and short terms objectives. The long term is interested in maximize the NPV, what means in some cases not producing at the full potential. While the short time is concerned on maximize production.

Then, to accommodate such conflicting interest, Van Essen et al. (2011) proposed a hierarchical optimization, in which the NPV is the primary objective and short time production, the secondary. This method takes advantage of the extra degree of freedom present in the reservoir optimization due to the elevated number of variables (an issue currently faced by history matching). So, since the primary objective is maximized there still a margin to change the variables inside the space null of the Hessian matrix; however, this is, according to the authors, "computationally infeasible for realistically sized problems". In the same paper, the authors proposed an alternative method of an alternating sequence of optimizing the primary- and secondary-objective function. The disadvantage is the slow convergence because the primary objective is harmed during the secondary optimization since the NPV is not used as a constraint during this period (Van Essen et al. 2011). Later, C. Chen et al. (2012) proposed a incremental switching method in which they incorporated the primary objective (i.e. NPV) as a constraint to the secondary optimization by using augmented Lagrangian.

In a broader view, some studies proposed a multilevel approach inspired on the process industry, specially on the petrochemical sector (Saputelli et al. 2005, 2006; Foss et al. 2011). Although the reservoir is still seen as a whole, the making decision process is dived into layers, each one with different objectives, level of decision, and frequency of action. Figure 2.3 helps to understand this idea, each decision layers communicates with its immediate upper and lower layers, with the upper ones giving set-points and receiving constraints from the lowers.

As higher one goes in this hierarchy, the higher is the level of decision and lower is the frequency of decisions. The top level represent the highest level of one organization, which takes the very-long terms decisions like explore or not a new field. Right below, there is the "Asset Management" level, which is responsible for long

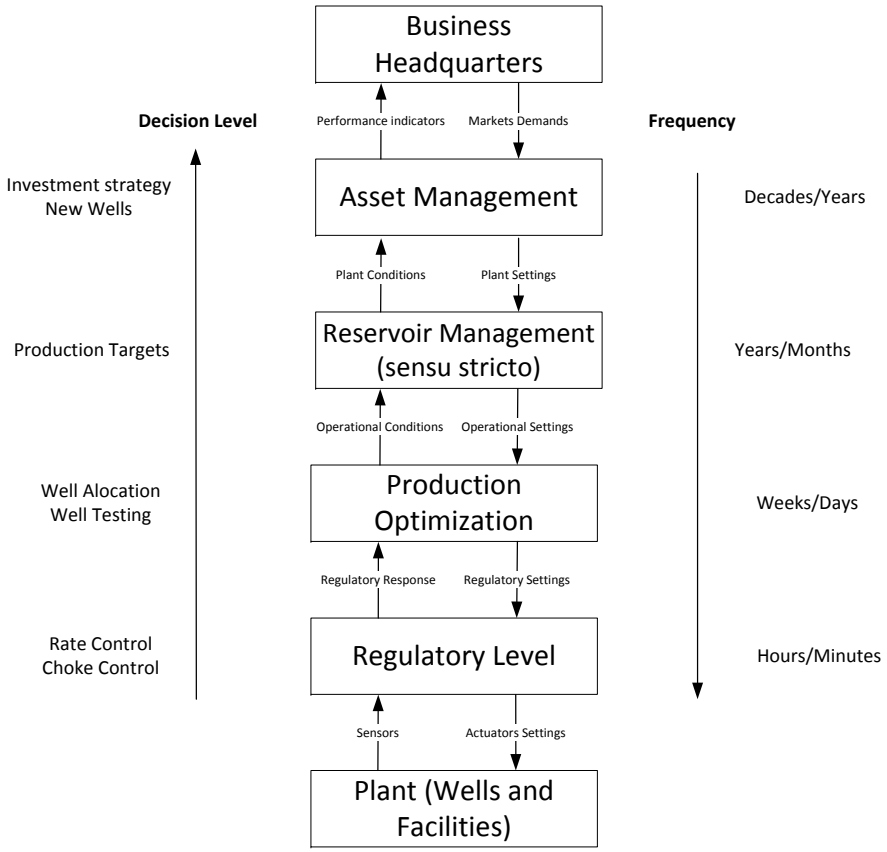

Figure 2.3: Multilevel hierarchy control (adapted from Saputelli et al. 2005, 2006)

term decisions, such drill a new well. After, one find the "Reservoir Management"[2], responsible for mid-term decisions; it defines production targets of a reservoir field well by well. The "Production optimization" layer is responsible short-time decisions; it major goal is reaching the set-points by, for instance, choosing if the well will produce either by the wellbore or by the tubing string. Finally, the last layer of decision is the "Regulatory level", which is completely automated regulated with no human intervention needed; it is responsible for very short-time decisions. Some examples of this level are: rate, pressure and choke control.

2. Here in the strict sense of the concept. The wide sense encompass all the layers.

The main goal of that multilevel structure is to adopt a more realistic and flexible approach. The reservoir management layer, thus, would not specify a specific set-point, but a maximum and minimum values instead. Leaving a certain degree of liberty for the production layer to operate under short-term consideration.

2.3.4 Reactive Control

The various methods of improving reservoir waterflooding through CLRM approach can be classified according to the following concepts:

- Passive control: In this approach, no feedback information is utilized. It is also known as an open-loop control. Example: pure optimal control.
- Active control: Employs the benefits of feedback (e.g. check if what is happening is equal to what was predict). It can be either reactive or proactive:
  - Reactive control: the algorithm changes the inputs of the control action in response to situations measured by sensors, such as arrival of a water front in the well. Example: close the well because of an high water cut.
  - Proactive control: the algorithm not only respond to measured values, but also to predicted situations. Example: nonlinear model predictive control.

The literature discussed so far treats the reservoir management as an optimization problem in a proactive control framework. Which employs mathematical algorithms, either gradient based like adjoint or gradient-free method like genetic algorithm or particle swarm, to optimize a predefined objective function (mostly NPV). This approach is known as "model based", since the optimizing function is a mathematical representation of the system. Therefore, the accuracy of such approach is heavily depend on the "quality" of such models. If the reservoir models do not capture all

the dynamical behaviors, the model based optimization will most likely be ineffective. Not to mention the fact that optimization are usually very computationally expensive.

Consequently, Addiego-Guevara et al. (2008) suggested that simple reactive control loop would improved production and mitigate reservoir uncertainty over a range of scenarios. They compared three control strategies applied thorough downhole valves (more details at section 2.4) in a simple conceptual reservoir model with a single horizontal production well underlaid by an aquifer. The first was a passive model-based control using pre-designed fixed control device; the second was an on-off reactive control responding to well water cut; the third was also a reactive control, but with variable control choking the completion depending to well water cut. According to their study, passive model control are riskier than actives because of the lack reliability of the reservoir model, with the active strategies always giving neutral or positive gains irrespective to model uncertainty.

Dilib et al. (2013) used a similar reservoir model to show that reactive feedback control yields to close-to-optimal gains in NPV compared with the theoretical optimal results when the reservoir is assumed to be known. Moreover, the algorithm was tested against unexpected reservoir behaviors to check its robustnesses; in contrast to Robust Optimization, which assumes that the reservoir uncertainties are captured by the several models. In a posterior work (Dilib et al. 2015), reactive feedback-control was tested in a more realistic reservoir: a thin oil-rim reservoir in North Sea underlain by an aquifer and also with a large gas cap. In this paper, they again compared two strategies: an open-loop using fixed inflow devices with a variable closed loop using inflow-control valves (ICVs). Similarly to their previous work, they also conclude that the closed loop feedback control is a safer strategy yielding to positive gains even under to unexpected reservoir behaviors. Unfortunately, they

did not investigate on/off control, neither compared their result with a model-based control to benchmark their claims.

Recently, Zhou et al. (2015) proposed a combined control, which have the advantages of both reactive and proactive control. They tested their algorithm in a simple 2D two phase reservoir with two horizontal well equipped with ICVs (one producer and one injector), and compared three strategies: simple reactive, simple proactive and combined. In the first strategy, the ICVs were proportionally choked according to well water cut measure by flow meters. In the second strategy, ICVs were proportionally choked according to the advance of the water front in the reservoir measured by reservoir-imaging sensors. The third strategy uses the water breakthrough as a switch between the two strategies: before the water breakthrough, proactive control to flatten the water front; after, reactive control to balance the water cuts inside each segment. The weak spot of this paper is the assumption of availability of reservoir-images sensors to perform proactive control; technology which is at young stages of development.

More traditional feedback controllers, such as proportional-integral-derivative (PID) and fuzzy controllers, have not yet been employed under the Closed loop Reservoir Management framework. On the other hand, Güyagüler et al. (2010) reported a study with three field process applications: first, locally average pressure maintenance by adjusting the voidage-replacement ratio between injectors and producers; second, prevention of gas/water conning; and third, average temperature maintenance within a region by flow control into the formation of a steam-assisted-gravity-drainage (SAGD) producer/injector pair. They assumed, however, a deterministic model (e.g. assuming complete knowledge of the reservoir); not taking, therefore, into account the reservoir uncertainties.

2.4 Smart Wells

Although a complete analysis of such technology is not the focus of this thesis (which is interested on the reservoir applications), this section will give a brief survey on advanced wells.

The development of "smart wells" (also refereed as "i-fields", "e-fields", and "digital fields") has potential to become a major breakthrough in the Reservoir Management field allowing not only more reliable downhole measurements, but also localized action (e.g. choke or shut selected zones with poor performance without intervention) (Gao et al. 2007).

There are two main types of smart wells: inflow control devices (ICDs) and interval-control valves (ICVs). An ICD is passive flow restriction installed as part of a well completion, which tries to equalize the reservoir inflow along the wellbore by balancing the completion and reservoir pressures differentials. Originally developed to reduce the heel-toe effect in horizontal wells, such devices require a good knowledge of the reservoir. Since the size of the restriction is set before or at the time of well completion, in other words, an ICD configuration is fixed once installed (Al-Khelaiwi et al. 2010).

An ICV is a downhole flow valve, which allows remote operation from the surface through electric, hydraulic, or electro-hydraulic actuation. An ICV, in contrast to ICD, allows actively control inflow, since the downhole flow path's diameter can be changed at any time without intervention, operating in either On/Off or even in a infinitely variable fashion (Al-Khelaiwi et al. 2010).

This key difference of flow control make ICVs the most preferable for Reservoir Management framework projects, despite the higher price. Specially in an uncertainty environment like reservoir, such flexibility of changing configuration helps to

mitigate risks and avoid expensive interventions.

In addition, a more evident benefit, ICVs can actively avoid early water breakthrough in a reactive control strategy by choking in response to increase water cut. And, in a extreme scenario, completely shut off fluid flow in the respective segment, but saving the well since multiples ICV can be installed in a single well.

This thesis will focus only in ICVs since it is the only equipment able to react to commands. It is considered, however, a perfect equipment not subject to failures. Evaluation of failures risk is a topic for future research.

2.4.1 Applications

Finally, although a relatively new technology, some important oil companies have been publishing papers describing their real case ICVs implementation. For instance, Saudi Aramco, a major enthusiast with 100 wells equipped with multiple downhole valves (Mubarak et al. 2009); Chevron in the Agbami deepwater oil field, offshore Nigeria (Adeyemo et al. 2009; Collins et al. 2012); Shell-BP partnership in the Na Kika project, deepwater Gulf of Mexico (Chacon et al. 2007); and Shell, mature assets in North Sea (Akram et al. 2001).

3. SUBSURFACE MODELING

This section presents the basic formulation of a Reservoir Simulator. Which is an essential part of Reservoir Management, allowing to predict scenarios and take decisions. In this thesis only the Black oil model with three phases (i.e. gas, oil, and water) will be considered. Which means that: although the components can be dissolved in each other depending on pressure or temperature, the hydrocarbon fluid composition remains constant. The fluid flow through porous media presented in this chapter is based on the textbook by Z. Chen et al. (2006).

The steps to develop a reservoir simulator are presented in fig. 3.1. First, the physical reservoir will be depict by nonlinear partial differential equations according to first principles. Second, a discretization is performed to achieve nonlinear algebraic equations. The third step is linearizion by one of this methods: finite difference, finite element, or finite volume. This section will show only finite difference method, the most classical one. The last step is to solve a hepta-block-diagonal matrix (for a three dimensional case).

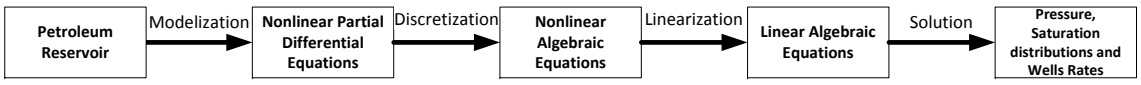

Figure 3.1: Multiphase simulator steps (adapted from Odeh 1982)

3.1 Reservoir Modeling

The black oil model is based on two primary physical principles: mass conservation of individual components or material balance, which gives "saturation distribu-

tion"; and momentum conservation, which gives "pressure"[1]. However, since mass interchange is allowed between oil and gas phases, only the total material balance is conserved and not within each phase.

3.1.1 Mass Balance Equations

The mass balance states for any close volume the difference between mass of inflow stream and mass of outflow stream is equal to the mass of fluid accumulation plus any external source (or minus any external sink) per unit time and volume.

$$Mass_{(inflow-outflow)} = Mass_{accumulation} \pm source/sink \tag{3.1}$$

Considering a infinitesimal element of volume V in the porous media. Then, the left hand side (LHS) of eq. (3.1) can be mathematically depicted as a surface integral of the mass flow rate over the region's boundary ($\oiint_{S(V)} -(\dot{m} \cdot \vec{n})\,\mathrm{d}S$). Where the mass flow rate of a fluid can be calculated by the multiplication of its density (ρ) times the fluid's velocity (v). The minus signal reflect the fact that the mass flow rate and the normal vector of the surface are in opposite senses, going into and out the control volume, respectively.

The accumulation term, in its turn, is the time rate of change of fluid mass inside the control volume ($\frac{\partial m}{\partial t}$). Where the mass of each component is calculated by the integral of the fluid density (ρ) times the respective phase saturation (S) times the effective volume, that is, the volume control multiplied by the rock's porosity (ϕ). Resulting, thus, in $\frac{\partial(\rho S \iiint_V \phi\,\mathrm{d}V)}{\partial t}$; but, because it is a continuously differentiable equation, the integration and the differentiation can be interchangeable.

1. Compositional models that allows changes in the fluids compositions uses a third principle: energy conversation, which gives "temperature distribution".

Therefore the material balance, eq. (3.1), can be written as:

$$\oiint_{S(V)} -(\rho v)\cdot\vec{n}\,\mathrm{d}S = \iiint_V \frac{\partial(\rho\phi S)}{\partial t}\,\mathrm{d}V - \iiint_V \tilde{m}\,\mathrm{d}V \tag{3.2}$$

where $\tilde{m}$ is mass flow rate per volume unit. Rearranging using the divergence theorem in the left hand side (LHS) of eq. (3.1):

$$\iiint_V -\nabla\cdot(\rho v)\,\mathrm{d}V = \iiint_V \frac{\partial(\rho\phi S)}{\partial t}\,\mathrm{d}V - \iiint_V \tilde{m}\,\mathrm{d}V \tag{3.3}$$

removing the integral symbols gives the so called fluid flow continuity equation for porous media:

$$-\nabla\cdot(\rho v) = \frac{\partial}{\partial t}(\rho\phi S) - \tilde{m} \tag{3.4}$$

Equation (3.4) is the general PDE pattern. And must be applied for each phase of the reservoir. So, from now on the lower- and uppercase letter subscripts indicates the three phases: water, oil and gas. For oil and water this is relatively simple:

$$-\nabla\cdot(\bar{\rho_o}v_o) = \frac{\partial}{\partial t}(\bar{\rho_o}\phi S_o) - \bar{\rho_o}\tilde{q_o} \tag{3.5}$$

$$-\nabla\cdot(\rho_w v_w) = \frac{\partial}{\partial t}(\rho_w\phi S_w) - \rho_w\tilde{q_w} \tag{3.6}$$

where $\bar{\rho_o}$ indicates the partial density of the oil in the oil phase.

However, the gas equation is slightly more complicated because gas can be dissolved in oil.

$$-\nabla\cdot(\rho_{dg}v_o + \rho_g v_g) = \frac{\partial}{\partial t}\left[(\rho_{dg}S_o + \rho_g S_g)\,\phi\right] - \rho_{dg}\tilde{q_o} - \rho_g\tilde{q}_{fg} \tag{3.7}$$

where ρ_{dg}, $\rho_{dg}\tilde{q_o}$ and $\rho_g\tilde{q}_{fg}$ represent, respectively, partial density of the gas component in oil phase, dissolved and free gas production.

3.1.2 Formation Volume Factor and Gas-Oil-Ratio

Formation Volume Factors (FVF) is common and useful concept which relates the phase volumes at surface conditions (SC) with reservoir conditions (RC), under the assumption of constant reservoir temperature.

$$B_o(p,T) = \frac{V_{o,RC}(p,T)}{V_{o,SC}} \tag{3.8}$$

$$B_w(p,T) = \frac{V_{w,RC}(p,T)}{V_{w,SC}} \tag{3.9}$$

$$B_g(p,T) = \frac{V_{g,RC}(p,T)}{V_{fg,SC}} \tag{3.10}$$

Another useful relationship for Black oil models is the dissolved gas-oil ratio, which correlates the amount of surface gas dissolved in the oil at any pressure:

$$R_s = \left[\frac{V_g}{V_o}\right]_{SC} \tag{3.11}$$

Relating the phase densities at reservoir conditions to the component densities at standard conditions:

$$\rho_o = \frac{\rho_{g,SC}R_s + \rho_{o,SC}}{B_o} \tag{3.12}$$

$$= \rho_{dg} + \bar{\rho_o} \tag{3.13}$$

$$\rho_w = \frac{\rho_{w,SC}}{B_w} \tag{3.14}$$

$$\rho_g = \frac{\rho_{g,SC}}{B_g} \tag{3.15}$$

Finally, after substituting eqs. (3.12) to (3.15) into eqs. (3.5) to (3.7) and also

dividing respectively by $\bar{\rho}_{o,SC}$, $\rho_{w,SC}$, and $\rho_{g,SC}$ yields to the mass conservation equations on standard volumes:

$$-\nabla \cdot \left(\frac{v_o}{B_o}\right) = \frac{\partial}{\partial t}\left(\frac{\phi S_o}{B_o}\right) - \frac{\tilde{q_o}}{B_o} \tag{3.16}$$

$$-\nabla \cdot \left(\frac{v_w}{B_w}\right) = \frac{\partial}{\partial t}\left(\frac{\phi S_w}{B_w}\right) - \frac{\tilde{q_w}}{B_w} \tag{3.17}$$

$$-\nabla \cdot \left(\frac{R_s}{B_o}v_o + \frac{v_g}{B_g}\right) = \frac{\partial}{\partial t}\left(\frac{R_s}{B_o}\phi S_o + \frac{1}{B_g}\phi S_g\right) - \frac{R_s}{B_o}\tilde{q}_o - \frac{1}{B_g}\tilde{q}_{fg} \tag{3.18}$$

3.1.3 Momentum Conservation

The second primary physical law is the momentum conservation, which for each phase is given by the Darcy's law in the porous media:

$$v = -\frac{k_r}{\mu}k(\nabla p - \rho g \nabla z) \tag{3.19}$$

where μ, p, k_r, k, g, and d are, respectively, the phase viscosity and pressure, relative and absolute permeability in the porous media, gravitational acceleration, and the depth.

So, substituting eq. (3.19) into eqs. (3.16) to (3.16) and defining "mobility ratio" (λ) as the ratio of effective permeability to phase viscosity and volume factor (e.g $\lambda_l = \frac{kr_l}{B_l \mu_l}k$, where λ_l is the mobility of phase l), yields to the general partial differential equation (PDE):

$$\nabla \cdot [\lambda_o(\nabla p_o - \rho_o g \nabla z)] = \frac{\partial}{\partial t}\left(\frac{\phi S_o}{B_o}\right) - \frac{\tilde{q_o}}{B_o} \tag{3.20}$$

$$\nabla \cdot [\lambda_w(\nabla p_w - \rho_w g \nabla z)] = \frac{\partial}{\partial t}\left(\frac{\phi S_w}{B_w}\right) - \frac{\tilde{q_w}}{B_w} \tag{3.21}$$

$$\nabla \cdot [R_s \lambda_o (\nabla p_o - \rho_o g \nabla z) + \lambda_g (\nabla p_g - \rho_g g \nabla z)] = \frac{\partial}{\partial t} \left(\frac{R_s}{B_o} \phi S_o + \frac{1}{B_g} \phi S_g \right) - \frac{R_s}{B_o} \tilde{q}_o - \frac{1}{B_g} \tilde{q}_{fg} \quad (3.22)$$

3.1.4 Primary Variables

There are 6 unknowns in eqs. (3.20) to (3.22), three phases pressures (p_o, p_g, p_w) plus three phases saturations (S_o, S_g, S_w). Therefore, more 3 equations are required to complete the system. One equation comes to the fact that the three phases jointly fill the void space, which is depicted by the equation:

$$S_o + S_w + S_g = 1 \quad (3.23)$$

The remaining two equation are given by the capillary pressures (e.g. the relation between the individual phase pressure):

$$p_{cow} = p_o - p_w \quad (3.24)$$

$$p_{cgo} = p_g - p_o \quad (3.25)$$

where water is assumed to be the wetting phase, oil the intermediate wetting phase, and gas the non wetting phase.

With this three extra equations, eqs. (3.20) to (3.22) can be rearranged to the final nonlinear partial differential equation form, with the primary variables as oil pressure (p_o), water saturation (S_w), and fractional gas saturation (S_g) as follows:

$$\nabla \cdot [\lambda_o (\nabla p_o - \rho_o g \nabla z)] = \frac{\partial}{\partial t} \left(\frac{\phi}{B_o} (1 - S_w - S_g) \right) - \frac{\tilde{q_o}}{B_o} \quad (3.26)$$

$$\nabla \cdot [\lambda_w (\nabla (p_o - p_{cow}) - \rho_w g \nabla z)] = \frac{\partial}{\partial t} \left(\frac{\phi}{B_w} S_w \right) - \frac{\tilde{q_w}}{B_w} \quad (3.27)$$

$$\nabla \cdot \left[R_s \lambda_o \left(\nabla p_o - \rho_o g \nabla z \right) + \lambda_g \left(\nabla \left(p_o - p_{cgo} \right) - \rho_g g \nabla z \right) \right]$$
$$= \frac{\partial}{\partial t} \left(\frac{R_s}{B_o} \phi \left(1 - S_w - S_g \right) + \frac{\phi}{B_g} S_g \right) - \frac{R_s}{B_o} \tilde{q}_o - \frac{1}{B_g} \tilde{q}_{fg} \quad (3.28)$$

3.1.5 Bubble Point (p_b) Threshold

In black oil model, the gas component can exist in both oil phase and gas phase. When the reservoir pressure is less than the bubble point pressure (p_b) of the oil phase (e.g. $p_o < p_b$), all three phases coexist and the free gas phase will present in the reservoir (i.e. $S_g \neq 0$). When this happens, the reservoir is refereed to as being in the saturated state. Then, the constraints for saturated reservoir are:

$$S_w + S_o + S_g = 1 \quad , \quad R_s > 0$$

On the other hand, when the reservoir pressure is greater than the bubble point pressure of the oil phase (e.g. $p_o > p_b$), all gas dissolves in the oil phase and there is no free gas in the reservoir(i.e. $S_g = 0$). In this case, the reservoir is said to be in the undersaturated state and the model called two phase flow. Then, the constraints for undersaturated reservoir are:

$$S_w + S_o = 1 \quad , \quad S_g = 0 \quad , \quad R_s = constant$$

and flow becomes only two-phase.

3.2 Discretization

Since nonlinear partial differential equations cannot be analytically solved, the next step is to perform a discretization to reach a set os nonlinear algebraic equations (fig. 3.1). Two types of discretization are necessary: in time and in space, and in both

cases the finite differences method is employed. The development of this subsection is based on Ertekin et al. (2001).

3.2.1 Spatial Discretization

To perform the spatial discretization, reservoir are divided into a million of thousands small grid blocks. Usually, each one has a cubic shape with dimensions of Δx, Δy, and Δz. Figure 3.2 shows a 2D representation of one grid block, with the centroid denoted as (x,y,z). Where the subscript (i, j, k) is the coordinate index that indicates the x, y and z direction respectively. Also, the distance between the centroids of middle cube and right cube is expressed as Δx_i^+, while the distance between middle cube and left cube is expressed as Δx_i^-.

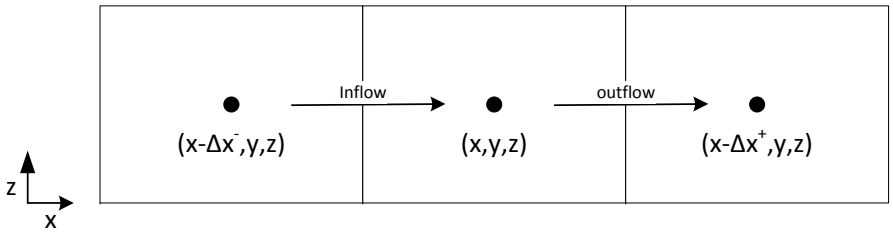

Figure 3.2: Flow across gridblocks in x-direction

From now on, whenever there is a plus or minus one in the subscript, it indicates the properties of adjacent gridblock. For instance $(i-1, j, k)$ indicates the properties of adjacent gridblock in negative x direction, while $(i+1, j, k)$ indicates the properties of adjacent gridblock in positive x direction. On the other hand, a plus or minus one half indicates the average property at the interface of two adjacent gridblock. For instance,$(i+\frac{1}{2}, j, k)$ indicates the average property at the interface of two adjacent gridblock in positive x direction, while the subscript $(i-\frac{1}{2}, j, k)$ indicates the

properties at the interface of two adjacent gridblock in negative x direction. Similar interpretation is extended to y and z directions.

The mass flux across the interface in x direction can be written as:

$$(\rho v_x)_{x-\frac{\Delta x}{2},y,z} \quad , \quad (\rho v_x)_{x+\frac{\Delta x}{2},y,z} \tag{3.29}$$

And the pressure differences gradient in x direction are:

$$\frac{p_{ox+\Delta x^+,y,z} - p_{ox,y,z}}{\Delta x^+} \quad , \quad \frac{p_{ox-\Delta x^-,y,z} - p_{ox,y,z}}{\Delta x^-} \tag{3.30}$$

Spatial discretization of conservation equation for water phase

Because the discretization steps for all three phases (i.e. water, oil and gas) are similar, only the water equation will be demonstrated in detail.

Firstly, one need to expand the vector differential operator (∇) in a specific coordinate system. In this thesis the cartesian system will be used, so $\nabla = \frac{\partial}{\partial x} + \frac{\partial}{\partial y} + \frac{\partial}{\partial z}$. Therefore the left hand side of eq. (3.27) can be written as follows:

$$\begin{aligned} \nabla \cdot \left[\lambda_w \left(\nabla \left(p_o - p_{cow}\right) - \rho_w g \nabla z\right)\right] \triangleq & \frac{\partial}{\partial x}\left[\lambda_{wx}\left(\frac{\partial p_o}{\partial x} - \frac{\partial p_{cow}}{\partial x} - \rho_w g \frac{\partial z}{\partial x}\right)\right] \\ & + \frac{\partial}{\partial y}\left[\lambda_{wy}\left(\frac{\partial p_o}{\partial y} - \frac{\partial p_{cow}}{\partial y} - \rho_w g \frac{\partial z}{\partial y}\right)\right] \\ & + \frac{\partial}{\partial z}\left[\lambda_{wz}\left(\frac{\partial p_w}{\partial z} - \frac{\partial p_{cow}}{\partial z} - \rho_w g \frac{\partial z}{\partial z}\right)\right] \end{aligned} \tag{3.31}$$

Then, assuming no potential energy along both x and y direction (i.e. $\frac{\partial z}{\partial x}$ and $\frac{\partial z}{\partial y}$ equal to zero) and applying the concepts of eqs. (3.29) to (3.30) yields the discretiza-

tion of the phase flux in x, y and z directions for water phase:

$$\frac{\partial}{\partial x}\left[\lambda_{wx}\left(\frac{\partial p_o}{\partial x}-\frac{\partial p_{cow}}{\partial x}-\rho_w g\frac{\partial z}{\partial x}\right)\right] \triangleq \frac{1}{\Delta x_i}\left(\lambda_{w i+\frac{1}{2},j,k}\frac{p_{oi+1,j,k}-p_{oi,j,k}}{\Delta x_i^+}+\lambda_{w i-\frac{1}{2},j,k}\frac{p_{oi-1,j,k}-p_{oi,j,k}}{\Delta x_i^-}\right) \quad (3.32)$$

$$\frac{\partial}{\partial y}\left[\lambda_{wy}\left(\frac{\partial p_o}{\partial y}-\frac{\partial p_{cow}}{\partial y}-\rho_w g\frac{\partial z}{\partial y}\right)\right] \triangleq \frac{1}{\Delta y_i}\left(\lambda_{w i,j+\frac{1}{2},k}\frac{p_{oi,j+1,k}-p_{oi,j,k}}{\Delta y_i^+}+\lambda_{w i,j-\frac{1}{2},k}\frac{p_{oi,j-1,k}-p_{oi,j,k}}{\Delta y_i^-}\right) \quad (3.33)$$

$$\begin{aligned}\frac{\partial}{\partial z}\left[\lambda_{wz}\left(\frac{\partial p_w}{\partial z}-\frac{\partial p_{cow}}{\partial z}-\rho_w g\frac{\partial z}{\partial z}\right)\right] &\triangleq \frac{1}{\Delta z_i}\left(\lambda_{w i,j,k+\frac{1}{2}}\frac{p_{oi,j,k+1}-p_{oi,j,k}}{\Delta z_i^+}+\lambda_{w i,j,k-\frac{1}{2}}\frac{p_{oi,j,k-1}-p_{oi,j,k}}{\Delta z_i^-}\right.\\ &\left.-\lambda_{w i,j,k+\frac{1}{2}}\gamma_{w i,j,k+\frac{1}{2}}\frac{z_{i,j,k+1}-z_{i,j,k}}{\Delta z_i^+}-\lambda_{w i,j,k-\frac{1}{2}}\gamma_{w i,j,k-\frac{1}{2}}\frac{z_{i,j,k-1}-z_{i,j,k}}{\Delta z_i^-}\right) \quad (3.34)\end{aligned}$$

where, $\gamma = \rho g$.

Combining the eqs. (3.32) to (3.34) yields the discretization of Darcy's term for

water conservation equations:

$$\begin{aligned}
&\nabla \cdot \left[\lambda_w \left(\nabla \left(p_o - p_{cow}\right) - \rho_w g \nabla z\right)\right] \triangleq \\
&\qquad \frac{1}{\Delta x_i}\left(\lambda_{wi+\frac{1}{2},j,k}\frac{p_{oi+1,j,k}-p_{oi,j,k}}{\Delta x_i^+} + \lambda_{wi-\frac{1}{2},j,k}\frac{p_{oi-1,j,k}-p_{oi,j,k}}{\Delta x_i^-}\right) \\
&\quad + \frac{1}{\Delta y_i}\left(\lambda_{wi,j+\frac{1}{2},k}\frac{p_{oi,j+1,k}-p_{oi,j,k}}{\Delta y_i^+} + \lambda_{wi,j-\frac{1}{2},k}\frac{p_{oi,j-1,k}-p_{oi,j,k}}{\Delta y_i^-}\right) \\
&\quad + \frac{1}{\Delta z_i}\left(\lambda_{wi,j,k+\frac{1}{2}}\frac{p_{oi,j,k+1}-p_{oi,j,k}}{\Delta z_i^+} + \lambda_{wi,j,k-\frac{1}{2}}\frac{p_{oi,j,k-1}-p_{oi,j,k}}{\Delta z_i^-}\right. \\
&\left.-\lambda_{wi,j,k+\frac{1}{2}}\gamma_{wi,j,k+\frac{1}{2}}\frac{z_{i,j,k+1}-z_{i,j,k}}{\Delta z_i^+} - \lambda_{wi,j,k-\frac{1}{2}}\gamma_{wi,j,k-\frac{1}{2}}\frac{z_{i,j,k-1}-z_{i,j,k}}{\Delta z_i^-}\right) \quad (3.35)
\end{aligned}$$

Spatial discretization of conservation equation for oil phase

Similarly, the discretization oil flux (left hand side of eq. (3.26)) term can be extended as:

$$\begin{aligned}
&\nabla \cdot \left[\lambda_o \left(\nabla p_o - \rho_o g \nabla z\right)\right] \triangleq \\
&\qquad \frac{1}{\Delta x_i}\left(\lambda_{oi+\frac{1}{2},j,k}\frac{p_{oi+1,j,k}-p_{oi,j,k}}{\Delta x_i^+} + \lambda_{oi-\frac{1}{2},j,k}\frac{p_{oi-1,j,k}-p_{oi,j,k}}{\Delta x_i^-}\right) \\
&\quad + \frac{1}{\Delta y_i}\left(\lambda_{oi,j+\frac{1}{2},k}\frac{p_{oi,j+1,k}-p_{oi,j,k}}{\Delta y_i^+} + \lambda_{oi,j-\frac{1}{2},k}\frac{p_{oi,j-1,k}-p_{oi,j,k}}{\Delta y_i^-}\right) \\
&\quad + \frac{1}{\Delta z_i}\left(\lambda_{oi,j,k+\frac{1}{2}}\frac{p_{oi,j,k+1}-p_{oi,j,k}}{\Delta z_i^+} + \lambda_{oi,j,k-\frac{1}{2}}\frac{p_{oi,j,k-1}-p_{oi,j,k}}{\Delta z_i^-}\right. \\
&\left.-\lambda_{oi,j,k+\frac{1}{2}}\gamma_{oi,j,k+\frac{1}{2}}\frac{z_{i,j,k+1}-z_{i,j,k}}{\Delta z_i^+} - \lambda_{oi,j,k-\frac{1}{2}}\gamma_{oi,j,k-\frac{1}{2}}\frac{z_{i,j,k-1}-z_{i,j,k}}{\Delta z_i^-}\right) \quad (3.36)
\end{aligned}$$

Spatial discretization of conservation equation for gas phase

For the discretization of gas conservation (left hand side of eq. (3.28)) there is an additional term $(R_s\lambda_o\left(\nabla p_o - \rho_o g \nabla z\right))$ which represents the gas components in oil phase must be considered. Their derivation in x, y and z-directions are shown

respectively as follows:

$$\frac{\partial}{\partial x}\left[R_s\lambda_{ox}\left(\frac{\partial p_o}{\partial x}-\gamma_o\frac{\partial z}{\partial x}\right)\right]$$
$$=\frac{1}{\Delta x_i}\left[(R_s\lambda_o)_{i+\frac{1}{2},j,k}\,\frac{p_{oi+1,j,k}-p_{oi,j,k}}{\Delta x_i^+}+(R_s\lambda_o)_{i-\frac{1}{2},j,k}\,\frac{p_{oi-1,j,k}-p_{oi,j,k}}{\Delta x_i^-}\right] \quad (3.37)$$

$$\frac{\partial}{\partial y}\left[R_s\lambda_{oy}\left(\frac{\partial p_o}{\partial y}-\gamma_o\frac{\partial z}{\partial y}\right)\right]$$
$$=\frac{1}{\Delta y_i}\left[(R_s\lambda_o)_{i,j+\frac{1}{2},k}\,\frac{p_{oi,j+1,k}-p_{oi,j,k}}{\Delta y_i^+}+(R_s\lambda_o)_{i,j-\frac{1}{2},k}\,\frac{p_{oi,j-1,k}-p_{oi,j,k}}{\Delta y_i^-}\right] \quad (3.38)$$

$$\frac{\partial}{\partial z}\left[R_s\lambda_{oz}\left(\frac{\partial p_o}{\partial z}-\gamma_o\frac{\partial z}{\partial z}\right)\right]$$
$$=\frac{1}{\Delta z_i}\left[(R_s\lambda_o)_{i,j,k+\frac{1}{2}}\,\frac{p_{oi,j,k+1}-p_{oi,j,k}}{\Delta z_i^+}+(R_s\lambda_o)_{i,j,k-\frac{1}{2}}\,\frac{p_{oi,j,k-1}-p_{oi,j,k}}{\Delta z_i^-}\right.$$
$$\left.-(R_s\lambda_o)_{i,j,k+\frac{1}{2}}\,\gamma_{oi,j,k+\frac{1}{2}}\,\frac{z_{i,j,k+1}-z_{i,j,k}}{\Delta z_i^+}-(R_s\lambda_o)_{i,j,k-\frac{1}{2}}\,\gamma_{oi,j,k-\frac{1}{2}}\,\frac{z_{i,j,k-1}-z_{i,j,k}}{\Delta z_i^-}\right] \quad (3.39)$$

Then combining eqs. (3.37) to (3.39) with a similar development as the one did in eq. (3.36) leads to the rather lengthy but complete spatial discretization of the

gas conservation equation:

$$
\begin{aligned}
&\nabla \cdot \left[R_s\lambda_o\left(\nabla p_o - \rho_o g \nabla z\right) + \lambda_g\left(\nabla\left(p_o - p_{cgo}\right) - \rho_g g \nabla z\right)\right] = \\
&\quad \frac{1}{\Delta x_i}\left[\left(R_s\lambda_o\right)_{i+\frac{1}{2},j,k}\frac{p_{oi+1,j,k}-p_{oi,j,k}}{\Delta x_i^+} + \left(R_s\lambda_o\right)_{i-\frac{1}{2},j,k}\frac{p_{oi-1,j,k}-p_{oi,j,k}}{\Delta x_i^-}\right] \\
&\quad + \frac{1}{\Delta y_i}\left[\left(R_s\lambda_o\right)_{i,j+\frac{1}{2},k}\frac{p_{oi,j+1,k}-p_{oi,j,k}}{\Delta y_i^+} + \left(R_s\lambda_o\right)_{i,j-\frac{1}{2},k}\frac{p_{oi,j-1,k}-p_{oi,j,k}}{\Delta y_i^-}\right] \\
&\quad + \frac{1}{\Delta z_i}\left[\left(R_s\lambda_o\right)_{i,j,k+\frac{1}{2}}\frac{p_{oi,j,k+1}-p_{oi,j,k}}{\Delta z_i^+} + \left(R_s\lambda_o\right)_{i,j,k-\frac{1}{2}}\frac{p_{oi,j,k-1}-p_{oi,j,k}}{\Delta z_i^-}\right. \\
&\quad \left. - \left(R_s\lambda_o\right)_{i,j,k+\frac{1}{2}}\gamma_{oi,j,k+\frac{1}{2}}\frac{z_{i,j,k+1}-z_{i,j,k}}{\Delta z_i^+} - \left(R_s\lambda_o\right)_{i,j,k-\frac{1}{2}}\gamma_{oi,j,k-\frac{1}{2}}\frac{z_{i,j,k-1}-z_{i,j,k}}{\Delta z_i^-}\right] \\
&\quad + \frac{1}{\Delta x_i}\left(\lambda_{g_{i+\frac{1}{2},j,k}}\frac{p_{oi+1,j,k}-p_{oi,j,k}}{\Delta x_i^+} + \lambda_{g_{i-\frac{1}{2},j,k}}\frac{p_{oi-1,j,k}-p_{oi,j,k}}{\Delta x_i^-}\right) \\
&\quad + \frac{1}{\Delta y_i}\left(\lambda_{g_{i,j+\frac{1}{2},k}}\frac{p_{oi,j+1,k}-p_{oi,j,k}}{\Delta y_i^+} + \lambda_{g_{i,j-\frac{1}{2},k}}\frac{p_{oi,j-1,k}-p_{oi,j,k}}{\Delta y_i^-}\right) \\
&\quad \frac{1}{\Delta z_i}\left(\lambda_{g_{i,j,k+\frac{1}{2}}}\frac{p_{oi,j,k+1}-p_{oi,j,k}}{\Delta z_i^+} + \lambda_{g_{i,j,k-\frac{1}{2}}}\frac{p_{oi,j,k-1}-p_{oi,j,k}}{\Delta z_i^-}\right. \\
&\quad + \left. -\lambda_{g_{i,j,k+\frac{1}{2}}}\gamma_{g_{i,j,k+\frac{1}{2}}}\frac{z_{i,j,k+1}-z_{i,j,k}}{\Delta z_i^+} - \lambda_{g_{i,j,k-\frac{1}{2}}}\gamma_{g_{i,j,k-\frac{1}{2}}}\frac{z_{i,j,k-1}-z_{i,j,k}}{\Delta z_i^-}\right)
\end{aligned}
\tag{3.40}
$$

3.2.2 Time Discretization

The time discretization derivation of accumulation term is based on the textbook by Ertekin et al. (2001). Again, only the water equation term is showed for simplicity. Applying the finite difference method to accumulation term in the right hand side of eq. (3.27) yields to:

$$
\frac{\partial}{\partial t}\left(\frac{\phi}{B_w}S_w\right) \approx \frac{1}{\Delta t}\left[\left(\phi S_w b_w\right)^{n+1} - \left(\phi S_w b_w\right)^n\right] \tag{3.41}
$$

where, for the sake of the simplicity, $b_w = \frac{1}{B_w}$ was defined and the superscript, n indicates the properties at the current time-step, while $n+1$ indicates the properties at the next time-step.

Then, to write eq. (3.41) as only a function of p_o and S_w, the term $(\phi b_w)^{n+1} S_w^n$ is added and subtracted:

$$\begin{aligned}\frac{\partial}{\partial t}\left(\frac{\phi}{B_w}S_w\right) &\approx \frac{1}{\Delta t}\left[(\phi S_w b_w)^{n+1} + (\phi b_w)^{n+1} S_w^n - (\phi b_w)^{n+1} S_w^n - (\phi S_w b_w)^n\right] \\ &\approx \frac{1}{\Delta t}\left[(\phi b_w)^{n+1}\left(S_w^{n+1} - S_w^n\right) + S_w^n\left[(\phi b_w)^{n+1} - (\phi b_w)^n\right]\right] \\ &\approx (\phi b_w)^{n+1}\Delta_t S_w + S_w^n \Delta_t (\phi b_w)\end{aligned} \tag{3.42}$$

where $\Delta_t(\cdot) = \frac{(\cdot)^{n+1} - (\cdot)^n}{\Delta_t}$.

Expanding the last term of eq. (3.42) yields to:

$$\frac{\partial}{\partial t}(\phi b_w S_w) \approx (\phi b_w)^{n+1}\Delta_t S_w + S_w^n\left(\phi^n \Delta_t b_w + b_w^{n+1}\Delta_t \phi\right) \tag{3.43}$$

But, because both porosity and formation volume factor are only functions of pressure, its respectively time difference functions can be expressed as follows:

$$\Delta_t \phi = \phi' \Delta_t p_o \tag{3.44}$$

$$\begin{aligned}\Delta_t b_w &= b'_w \Delta_t p_w \\ &= b'_w(\Delta_t p_o - \Delta_t p_{cow})\end{aligned} \tag{3.45}$$

where $\Delta_t p_{cow} = p'_{cow}\Delta_t S_w$. And b'_w, ϕ' and p'_{cow} are chord slops given by:

$$\phi' = \frac{\phi^{n+1} - \phi^n}{p_o^{n+1} - p_o^n} \tag{3.46}$$

$$b'_w = \frac{b_w^{n+1} - b_w^n}{p_w^{n+1} - p_w^n} \tag{3.47}$$

$$p'_{cow} = \frac{p_{cow}^{n+1} - p_{cow}^n}{S_w^{n+1} - S_w^n} \tag{3.48}$$

So, finally, substituting eqs. (3.44) to (3.45) into eq. (3.43) gives the discretized accumulation term for the water equation:

$$\begin{aligned}\frac{\partial}{\partial t}\left(\phi b_w S_w\right) &\approx \left(\phi b_w\right)^{n+1}\Delta_t S_w + S_w^n \phi^n b_w' \Delta_t p_o - S_w^n \phi^n b_w' p_{cow}' \Delta_t S_w + S_w^n b_w^{n+1}\phi' \Delta_t p_o \\ &\approx S_w^n\left[b_w^{n+1}\phi' + \phi^n b_w'\right]\Delta_t p_o + \left[\left(\phi b_w\right)^{n+1} - S_w^n \phi^n b_w' p_{cow}'\right]\Delta_t S_w \\ &\approx \beta_{wp}^* \Delta_t p_o + \beta_{wsw}^* \Delta_t S_w\end{aligned} \tag{3.49}$$

Similar derivation will lead to the discretized accumulation term, first term of the right hand side of eq. (3.26), for the oil equation:

$$\begin{aligned}\frac{\partial}{\partial t}\left[\frac{\phi\left(1-S_g-S_w\right)}{B_o}\right] &= \left(1-S_w-S_g\right)^n\left({b_o}^n\phi' + \phi^{n+1}b_o'\right)\Delta_t p_o \\ &\quad - \left(\phi b_o\right)^{n+1}\Delta_t S_w - \left(\phi b_o\right)^{n+1}\Delta_t S_g \\ &= \beta_{op}^*\Delta_t p_o + \beta_{osw}^*\Delta_t S_w + \beta_{osg}^*\Delta_t S_g\end{aligned} \tag{3.50}$$

Finally, the accumulation term in gas conservation formulation, first term of the right hand side of eq. (3.28), is expended as:

$$\begin{aligned}&\frac{\partial}{\partial t}\left[\frac{R_S\phi\left(1-S_g-S_w\right)}{B_o} + \frac{\phi S_g}{B_g}\right] \\ &\quad = \left[\left(b_o\phi S_o\right)^n R_s' + \left(b_g^n S_g^n + R_s^{n+1}S_o^n b_o^n\right)\phi' + \phi^{n+1}\left(R_s^{n+1}S_o^n b_o' + S_g^n b_g'\right)\right]\Delta_t p_o \\ &\quad - R_s^{n+1}\left(b_o\phi\right)^{n+1}\Delta_t S_w + \left[\left(b_g\phi\right)^{n+1} + \phi^{n+1}S_g^n b_g' p_{cgo}' - R_s^{n+1}\left(b_o\phi\right)^{n+1}\right]\Delta_t S_g\end{aligned} \tag{3.51}$$

and thus

$$\frac{\partial}{\partial t}\left[\frac{R_S\phi\left(1-S_g-S_w\right)}{B_o} + \frac{\phi S_g}{B_g}\right] = \beta_{gp}^*\Delta_t p_o + \beta_{gsw}^*\Delta_t S_w + \beta_{gsg}^*\Delta_t S_g \tag{3.52}$$

3.2.3 Well Modeling

The last part of the discretization step is to add the well model,. which can be done through the Peaceman's equations (Ertekin et al. 2001). This equation, however, is only valid for vertical wells, being not applicable for more complex configurations (e.g. fracturing).

$$q_w^* = WI_w(p_{w_{wc}}^{n+1} - p_{wf}) \tag{3.53}$$

where the subscript wc indicates the grid blocks where the well is placed. And WI_w is well index, which is defined as follows:

$$WI_w = -\frac{2\pi k_{rw} h\sqrt{k_x k_y}}{\mu_w B_w \left[ln(\frac{r_0}{r_w}) + s\right]} \tag{3.54}$$

where k_x is absolute permeability in x-direction, k_y absolute is permeability in y-direction, h is thickness of gridblock, r_w is wellbore radius, s is the skin factor and r_o is the the equivalent radius.

According to Ertekin et al. (2001) equivalent radius equivalent wellblock radius, at which the steady-state pressure in the reservoir is equal to the wellblock pressure, $p_{i,j,k}$), is given by:

$$r_0 = 0.28\frac{\sqrt{\left[\left(\frac{k_y}{k_x}\right)^{\frac{1}{2}}(\Delta x)^2\right] + \left[\left(\frac{k_x}{k_y}\right)^{\frac{1}{2}}(\Delta y)^2\right]}}{\left(\frac{k_y}{k_x}\right)^{\frac{1}{4}} + \left(\frac{k_x}{k_y}\right)^{\frac{1}{4}}} \tag{3.55}$$

3.2.4 The Black Oil Matrix Equation

The equations for the discretized black oil model are extremely lengthy and difficult to maneuver. However, with few additional step they can be re-written in a

matrix form to become more friendly.

Since the procedure is rather similar for the three phases equation, only the oil phase will be treat in some detail. Then, combing the final discretized formulations eqs. (3.36) and (3.50) and multiplying everything by the grid block volume ($V_{gb} = \Delta x_i \Delta y_i \Delta z_i$) yields to:

$$\begin{aligned}
&\frac{V_{gb}}{\Delta x_i}\left(\lambda_{oi+\frac{1}{2},j,k}\frac{p_{oi+1,j,k}-p_{oi,j,k}}{\Delta x_i^+}+\lambda_{oi-\frac{1}{2},j,k}\frac{p_{oi-1,j,k}-p_{oi,j,k}}{\Delta x_i^-}\right)\\
&+\frac{V_{gb}}{\Delta y_i}\left(\lambda_{oi,j+\frac{1}{2},k}\frac{p_{oi,j+1,k}-p_{oi,j,k}}{\Delta y_i^+}+\lambda_{oi,j-\frac{1}{2},k}\frac{p_{oi,j-1,k}-p_{oi,j,k}}{\Delta y_i^-}\right)\\
&+\frac{V_{gb}}{\Delta z_i}\left(\lambda_{oi,j,k+\frac{1}{2}}\frac{p_{oi,j,k+1}-p_{oi,j,k}}{\Delta z_i^+}+\lambda_{oi,j,k-\frac{1}{2}}\frac{p_{oi,j,k-1}-p_{oi,j,k}}{\Delta z_i^-}\right.\\
&\left.-\lambda_{oi,j,k+\frac{1}{2}}\gamma_{oi,j,k+\frac{1}{2}}\frac{z_{i,j,k+1}-z_{i,j,k}}{\Delta z_i^+}-\lambda_{oi,j,k-\frac{1}{2}}\gamma_{oi,j,k-\frac{1}{2}}\frac{z_{i,j,k-1}-z_{i,j,k}}{\Delta z_i^-}\right)\\
&\qquad = V_{gb}\left(1-S_w-S_g\right)^n\left({b_o}^n\phi'+\phi^{n+1}b_o'\right)\Delta_t p_o - V_{gb}\left(\phi b_o\right)^{n+1}\Delta_t S_w\\
&\qquad\qquad - V_{gb}\left(\phi b_o\right)^{n+1}\Delta_t S_g - \frac{V_{gb}}{B_o}\tilde{q}_o \quad (3.56)
\end{aligned}$$

Then, defining Interblock Trasmissibility as: $T_{oi\pm\frac{1}{2},j,k} = \left(\frac{A}{\Delta x_i^{\mp}}\lambda_{oi\pm\frac{1}{2},j,k}\right)$, and considering a orthogonal grid (i.e $\Delta x_i^+ = \Delta x_i^-$), eq. (3.56) becomes:

$$\begin{aligned}
&T_{oi+\frac{1}{2},j,k}(p_{oi+1,j,k}-p_{oi,j,k})+T_{oi-\frac{1}{2},j,k}(p_{oi-1,j,k}-p_{oi,j,k})\\
&+T_{oi,j+\frac{1}{2},k}(p_{oi,j+1,k}-p_{oi,j,k})+T_{oi,j-\frac{1}{2},k}(p_{oi,j-1,k}-p_{oi,j,k})\\
&+T_{oi,j,k+\frac{1}{2}}(p_{oi,j,k+1}-p_{oi,j,k})+T_{oi,j,k-\frac{1}{2}}(p_{oi,j,k-1}-p_{oi,j,k})\\
&-T_{oi,j,k+\frac{1}{2}}\gamma_{oi,j,k+\frac{1}{2}}(z_{i,j,k+1}-z_{i,j,k})-T_{oi,j,k-\frac{1}{2}}\gamma_{oi,j,k-\frac{1}{2}}(z_{i,j,k-1}-z_{i,j,k})\\
&\qquad = \beta_{op}\Delta_t p_o - \beta_{osw}\Delta_t S_w - \beta_{osg}\Delta_t S_g - q_o^* \quad (3.57)
\end{aligned}$$

Finally, eq. (3.57) may be expressed in a matrix form:

$$\mathbf{T}\vec{X} = \mathbf{D}\left(\frac{\partial \vec{X}}{\partial t}\right) - \vec{G} - \vec{Q} \tag{3.58}$$

Since eq. (3.58) is a nonlinear differential equation, one of the following methods may be applied to transform it in a nonlinear algebraic equation: lagging coefficient, simultaneous solution (SS) method, the implicit pressure explicit saturation (IMPES) method, and the sequential solution (SEQ) method. Here, the simultaneous solution (SS) method (also called as Fully Implicit) will be presented because it is the most powerful one, yet more computationally expensive than the other. Therefore, eq. (3.58) reduces to (abusing of the notation as $D = \frac{D}{\Delta t}$):

$$\mathbf{T}^{n+1}\vec{X}^{\,n+1} - \mathbf{D}^{n+1}\left(\vec{X}^{\,n+1} - \vec{X}^{\,n}\right) - \vec{G}^{\,n+1} - \vec{Q}^{\,n+1} = 0 \tag{3.59}$$

where:

$\vec{X} \Rightarrow$ State variables

$D \Rightarrow$ Accumulation matrix

$T \Rightarrow$ Transmissibility matrix

$\vec{G} \Rightarrow$ Vector of gravity terms

$\vec{Q} \Rightarrow$ Source vector

The definition of these vectors and matrices follow. Firstly, the states variables,

which represents the unknowns:

$$\vec{X} = \left(\vec{X}_1, \vec{X}_2, \vec{X}_3 \ldots \vec{X}_N\right)^T \tag{3.60}$$

$$\vec{X}_n = \left[S_{wn}, S_{g_n}, p_{on}\right]^T \tag{3.61}$$

where $n = 1, 2, 3, \ldots, N$. And "N" is the total number of grid blocs.

Next the source vector is defined as follow::

$$\vec{Q} = \left(\vec{Q}_1, \vec{Q}_2, \vec{Q}_3 \ldots \vec{Q}_N\right)^T \tag{3.62}$$

$$\vec{Q}_n = \left[q^n_{wn}, q^n_{g\,n}, q^n_{o\,n}\right]^T \tag{3.63}$$

The vector of gravity terms has the following shape:

$$\vec{G} = \left(\vec{G}_1, \vec{G}_2, \vec{G}_3 \ldots \vec{G}_N\right)^T \tag{3.64}$$

$$\vec{G}_n = \begin{bmatrix} \sum\limits_{m\in\psi_n} \left(T_w\gamma_w\right)^n_{n,m} \Delta_m z \\ \sum\limits_{m\in\psi_n} \left(T_g\gamma_g + T_o R_s \gamma_o\right)^n_{n,m} \Delta_m z \\ \sum\limits_{m\in\psi_n} \left(T_o\gamma_o\right)^n_{n,m} \Delta_m z \end{bmatrix} \tag{3.65}$$

The accumulation matrix is block diagonal matrix in a form as:

$$\mathbf{D} = diag\begin{pmatrix} \mathbf{D}_1 & \mathbf{D}_2 & \mathbf{D}_3 & \ldots & \mathbf{D}_N \end{pmatrix} \tag{3.66}$$

$$\mathbf{D}_n = \begin{bmatrix} \beta_{wsw_n} & \beta_{wsg_n} & \beta_{wp_n} \\ \beta_{gsw_n} & \beta_{gsg_n} & \beta_{gp_n} \\ \beta_{osw_n} & \beta_{osg_n} & \beta_{op_n} \end{bmatrix} \tag{3.67}$$

where the parameters of the matrix $\mathbf{D}_n$ are:

$$\beta_{wsw} = \frac{V_{gb}}{\Delta t}\left[(\phi b_w)^{n+1} - S_w^n \phi^n b'_w p'_{cow}\right] \tag{3.68}$$

$$\beta_{wsg} = 0 \tag{3.69}$$

$$\beta_{wp} = \frac{V_{gb}}{\Delta t}\left[b_w^{n+1}\phi' + \phi^n b'_w\right] \tag{3.70}$$

$$\beta_{gsw} = -\frac{V_{gb}}{\Delta t} R_s^{n+1}\left(b_o\phi\right)^{n+1} \tag{3.71}$$

$$\beta_{gsg} = \frac{V_{gb}}{\Delta t}\left[(b_g\phi)^{n+1} + \phi^{n+1} S_g^n b'_g p'_{cgo} - R_s^{n+1}\left(b_o\phi\right)^{n+1}\right] \tag{3.72}$$

$$\beta_{gp} = \frac{V_{gb}}{\Delta t}\left[(b_o\phi S_o)^n R'_s + \left(b_g^n S_g^n + R_s^{n+1} S_o^n b_o^n\right)\phi' + \phi^{n+1}\left(R_s^{n+1} S_o^n b'_o + S_g^n b'_g\right)\right] \tag{3.73}$$

$$\beta_{osw} = \beta_{osg} = -\frac{V_{gb}}{\Delta t}\left(\phi b_o\right)^{n+1} \tag{3.74}$$

$$\beta_{op} = \frac{V_{gb}}{\Delta t}\left(1 - S_w - S_g\right)^n \left({b_o}^n \phi' + \phi^{n+1} b'_o\right) \tag{3.75}$$

Finally, the transmissibibity matrix has a block structure. In which the sub-matrices of the block off-diagonals terms are defined as follows:

$$\mathbf{T}_{n,m} = \begin{bmatrix} -\left(T_w p'_{cow}\right)_{n,m}^n & 0 & \left(T_w\right)_{n.m}^n \\ 0 & \left(T_g p'_{cog}\right)_{n,m}^n & \left(T_g + T_o R_s\right)_{n,m}^n \\ 0 & 0 & \left(T_o\right)_{n.m}^n \end{bmatrix} \tag{3.76}$$

where $m \in \psi_n$ And the block diagonals terms are:

$$\mathbf{T}_{n,n} = -\sum_{m \in \psi_n} \mathbf{T}_{n,m} \tag{3.77}$$

3.3 Linearization

Since the final discretized equation, eq. (3.59), of the conservation equation for water, oil and gas phase are nonlinear algebraic equations, a linearization method is

required to solve these equations. In this study the classic Newton-Raphson method is used. Which is iterative method for finding better approximations to the roots of a real-valued function.

Recalling eq. (3.59) and defining the residual vector as:

$$R = \mathbf{T}^{n+1}\vec{X}^{\,n+1} - \mathbf{D}^{n+1}\left(\vec{X}^{\,n+1} - \vec{X}^{\,n}\right) - \vec{G}^{\,n+1} - \vec{Q}^{\,n+1} = 0 \tag{3.78}$$

Then, expanding the residual function by Taylor's theorem:

$$R(\vec{X}^{\,\nu+1}) = R(\vec{X}^{\,\nu}) + \mathbf{J}(\vec{X}^{\,\nu+1} - \vec{X}^{\,\nu}) + O(h^2) = 0 \tag{3.79}$$

where $O(h^2)$ can be ignored if the difference $(\vec{X}^{\,\nu+1} - \vec{X}^{\,\nu})$ is small. The Jacobian matrix, J, is a block structured matrix similar to the transmissibility matrix,

$$J_{n,m} = \begin{bmatrix} \frac{\partial R_{w_n}}{\partial S_{w_m}} & \frac{\partial R_{w_n}}{\partial S_{g_m}} & \frac{\partial R_{w_n}}{\partial S_{o_m}} \\ \frac{\partial R_{g_n}}{\partial S_{w_m}} & \frac{\partial R_{g_n}}{\partial S_{g_m}} & \frac{\partial R_{g_n}}{\partial S_{o_m}} \\ \frac{\partial R_{o_n}}{\partial S_{w_m}} & \frac{\partial R_{o_n}}{\partial S_{g_m}} & \frac{\partial R_{o_n}}{\partial S_{o_m}} \end{bmatrix} \tag{3.80}$$

Because R should be equal to zero, $R(\vec{X}^{\,\nu+1})$ can be eliminated, then eq. (3.79) becomes:

$$\vec{X}^{\,\nu+1} = \vec{X}^{\,\nu} + \delta \tag{3.81}$$

where delta is linear solution of $J\delta = -R(\vec{X}^{\,\nu})$.

This process is iteratively repeated until solution converges to a minimum value of tolerance, as depicted in the flowchart showed in fig. 3.3.

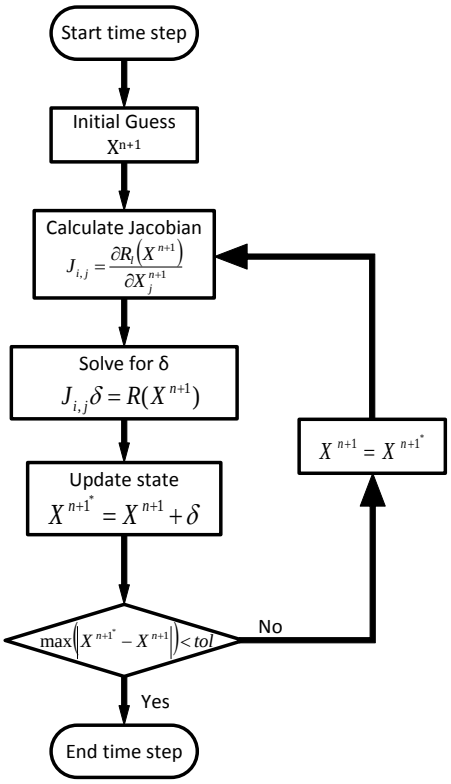

Figure 3.3: Newthon-Raphson flowchart

3.4 Inflow Control Valve Modeling

Since all simulation were performed in the commercial simulator Eclipse from Schulumberger, the discussion of this sub section is based on its manuals (Schlumberger 2014a).

Internal Control Valves are represented by sub-critical valves in the simulator by the keyword WSEGVALV. Mathematically speaking, a pressure drop is calculated using a homogeneous model of sub-critical flow through a pipe containing a constriction. Then added to the well model.

Such a pressure drop is formed by two factor: one that accounts the effects of the constriction and another that accounts for any additional friction pressure loss;

as shown in eq. (3.82).

$$\delta P = \delta P_{cons} + \delta P_{fric} \tag{3.82}$$

The first part, the constriction factor is calculated as:

$$\delta P_{cons} = C_\mu \frac{\rho v_c^2}{2C_v^2} \tag{3.83}$$

where C_μ is a units conversion constant, ρ is the density of the fluid mixture, v_c is the flow velocity of the mixture through the constriction, and C_v is a dimensionless flow coefficient for the valve.

The second term of eq. (3.82), the friction pressure loss is calculated as:

$$\delta P_{fric} = 2C_\mu f \frac{L}{D} \rho v_p^2 \tag{3.84}$$

where f is the Fanning friction factor, L is the additional length of piping in the segment, D is the diameter of the pipe (not the constriction), and v_p is the flow velocity of the mixture through the pipe.

An important relation must be point out between v_c and v_p and their respective cross-section areas, of the constriction and of the pipe, given by the following equation:

$$v_c A_c = v_p A_p = q_m \tag{3.85}$$

where q_m is defined as the local volumetric flow rate of the mixture

Substituting eq. (3.85) into eq. (3.83), the constriction flow pressure drop becomes:

$$\delta P_{cons} = C_\mu \frac{\rho q_m^2}{2C_v^2 A_c^2} \tag{3.86}$$

where A_c is the cross-sectional area of the valve constriction and takes a minimum

value of 1.0E-10.

And the friction pressure loss part can be rewrite by substituting eq. (3.85) into eq. (3.84):

$$\delta P_{fric} = 2C_{\mu} f \frac{L}{D} \rho \frac{q_m^2}{A_p^c} \tag{3.87}$$

In conclusion, both terms - eqs. (3.86) and (3.87) - are related to volumetric flow through the constriction. Ultimately, by controlling the constriction area, A_c it is possible to changing the pressure loss through the ICV and then modifying the fluid production.

Finally, another definition is the base strength of the device K, with dimension of inverse area squared, from eq. (3.86).

$$K = \frac{C_{\mu}}{2C_v^2 A_c^2} \tag{3.88}$$

Such a definition is important because it will define a lower bound to cross-section area of the constriction, A_c. Because, when the strength of the valve is greater than 0.1 it will cause the valve to shut. Therefore:

$$A_{c_{min}} = \sqrt{\frac{C_{\mu}}{0.2C_v^2}} \tag{3.89}$$

The upper bound of A_C, on the other hand, is when the constriction cross-section area is equal to the pipe cross-section area. Which is given by the following relation regarding the tubing diameter, D:

$$A_{c_{max}} = \pi \left(\frac{D^2}{4} \right) \tag{3.90}$$

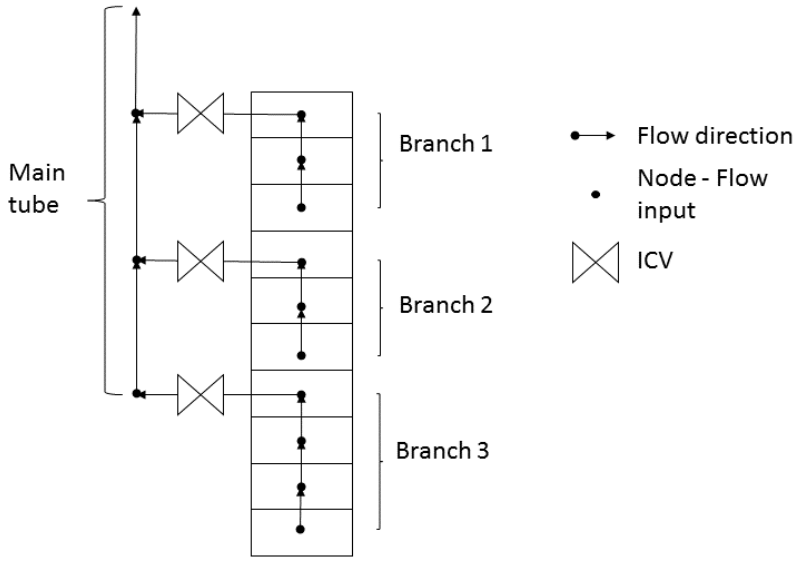

Figure 3.4: Multisegment well

3.4.1 Multisegment Wells

In order to properly modeling an ICV , the commercial reservoir simulator Eclipse has a special extension for multisegment well model (Schlumberger 2014b). In such kind of representation, the well bore is divided in independents segments. Each segment has one node from where the fluid flow into. Then, some segments are grouped in branchs which are connected to the main tube through one special segment where the ICV is located. Therefore, one ICV can control the flow of several segments depending on the configuration of the well. Figure 3.4 shows an example of a multisegment well with 3 ICVs allocated along a vertical well with 10 layers.

4. OPTIMIZATION

This section will present a brief overview of optimization methods and their important aspects used in the development of this thesis. Most of the theoretical work is based on Nocedal et al. (2006).

Optimization plays an important role in the decision making process, helping decision makers to choose between strategies that will maximize their goals, such as efficiency, profit, time, among others. However, there is no universal answer to all decision questions, requiring then, the use of several techniques, each of it fo a particular purpose or type of problem tailor.

Some general definitions, however, are common to all algorithms. The task of any optimization problem is to maximize or minimize an "Objective function" (represented here by J), defined as a quantitative measure of the performance of the system. Such a function is dependent on system variables (x), which are normally restricted by constraint functions (c_i), for example, maximum capital investment.

Maximizing or minimizing is the same type of problem. For instance, a function J can be maximized or minimized by just taking the negative $-J$.

Mathematically speaking, the formulation can be represented as follow:

$$\begin{aligned} \min_{x \in \mathbf{R}^n} \quad & J(x) \\ \text{subject to} \quad & c_i(x) \geq b_i, \ i = 1, \ldots, m. \end{aligned} \tag{4.1}$$

Several iterative algorithm have been develop through the years to solve eq. (4.1). Starting from an initial guess x_o, these algorithms generate a sequence of improved estimations until a certain requirement is achieve and a solution is, hopefully, found. According to the technique used to move from a previous iteration to the next one,

the optimization methods can be classified into two categories:

- Gradient-based algorithms. This type of algorithm uses the calculation of derivative and/or Hessian matrix (second derivative) to find the search direction. They are highly computationally efficient, but they need detailed knowledge about the system in order to calculate the derivatives.

- Gradient-free algorithms. This type of algorithm accumulate information from previous iteration to estimate the next one. For instance, artificial intelligence algorithms which are inspired by behaviors in nature such as inference, designing, thinking, and learning. Such algorithms are low computationally efficient, normally demanding thousands of simulations, but, on the other hand, can treat the reservoir simulator as a "black box".

4.1 Global and Local Optimization

For nonlinear problems, which is the case of reservoir simulation, there can exist several "local solutions", but only one is the lowest (or highest) objetive function value among all values, which is called "global solution". Such a problem does not happen in linear problems because only one solution exists. Figure 4.1 shows a simple example with three minimum, two locals and one global.

Recognition of a global solution is a daunting task, and even more difficult is to find such solutions. Then, for practical purposes, a local solution is acceptable given an almost infinite search of the global one.

This definition is important because gradient-based algorithms can be trapped in local solution. Since it is an iterative search, running from one point to other though derivative information, it is very important start as closes as possible of an global solution. This is not a trivial job, but an extremely important aspect of gradient-based algorithms.

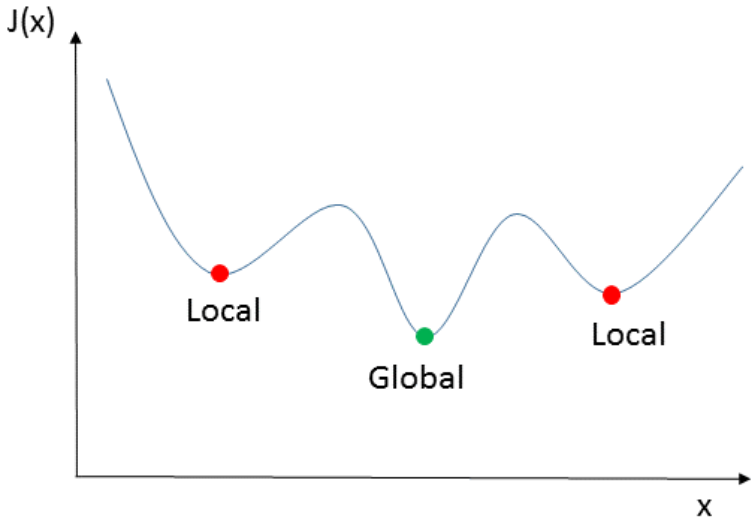

Figure 4.1: Difference between local and global solutions

Gradient-free algorithm are more suitable to find global solutions in the case of lack of knowledge of a good first guess, but there is no guarantee of that. In the end, it becomes a user choice and how much computational infrastructure one has.

4.2 Optimization in Commercial Reservoir Simulators

The use of gradient-free algorithm in commercial simulators is a relative easy task in terms of programming. The cost, however, maybe be too high for large scale applications. For instance, an application of genetic algorithm usually demands 100 iterations of 100 simulations each, thus a total of tens of thousands simulation are required in the optimization process. Adding verification and validation on th etop of that makes the computational time being in the order of days. This in the case of every parameter of the algorithm is right, which is not the usual case, then maybe more 2 or 3 optimizations will be performed. So, one simple case can easily demand 15 days.

Gradient-based optimizations, on the other hand, can be much faster. Their drawback is in the derivative calculation as numerical computational of the gradient is very often necessary. To do this end, there are basically three methods for calculation of the gradient:

- Numerical perturbation. It consist of small perturbations of the model parameters and calculation of the production responses. This method is easy implementable, but computationally expensive and thus unsuitable for large-scale optimization problem.

- Sensitivity equation. It consist of symbolic differentiation of the flow and transport equations. Although the fastest computational method, it is difficult to obtain analytical expressions for nonlinear problems.

- Adjoint method. It relies on optimal control theories and variational calculus. It is easy to implement, although it is a tedious process to code. It will be demonstrated in section 4.4.1, that adjoints are dependent on internal informations of the reservoir simulators, e.g. the Jacobian matrix of the residual vector - eq. (3.80), and thus, some of this information may not be accessible to users.

Fortunately, Eclipse Compositional Simulator - E300 - has a special extension of "optimization" which make the adjoint calculation within the simulator. This is one of the reason of all simulation of this thesis were implemented in Eclipse. Although such software is originally designed for volatile reservoir with operation point close to critical point (using multi-component mixtures to represent oil and gas phases and assuming that an equation of state (EoS) represent the composition of the reservoir fluids at specific temperatures and pressures), we simplify the calculus and the cases

by using a simple blackoil reservoir formulation. In this case, there is a keyword "BLACKOIL" that activates the black oil mode.

4.3 Optimization Algorithms

The optimization algorithms built in Eclipse are based on "*Line search strategy*" to move from a current point x_x to a new iterate x_{k+1}. In this strategy, the algorithm chooses a *search direction* p_k and searches by a *step lengh* α how much to move along this direction. This can be mathematically represented as follows:

$$x_{k+1} = x_k + \alpha_k p_k \tag{4.2}$$

Choosing an optimal step length, α, is time consuming and usually not necessary. So, an alternative is to try a limited set of generated values until the algorithm finds one that produces the minimum objective function value.

Two algorithms available to choose are "*Steepest descend*" and "*Nonlinear Conjugate Gradient*" (NLCG). They are different in the way they choose the search of direction. In any case, both methods require the evaluation of the gradient of the objective function. A more in deth discussion is given below.

4.3.1 Steepest Descend

In such method, the search direction is sought to be the negative gradient of the objective function at an specific iteration, $-\nabla f_k$. This is due to the fact that one can take the Taylor expansion of the objective function of the next iteration as:

$$\begin{aligned} J(x_{k+1}) &= J(x_k + \alpha p) \\ &= J(x_k) + \alpha p^T \nabla J_k + \frac{1}{2}\alpha^2 p^T \nabla^2 J(x_k + tp)p \end{aligned} \tag{4.3}$$

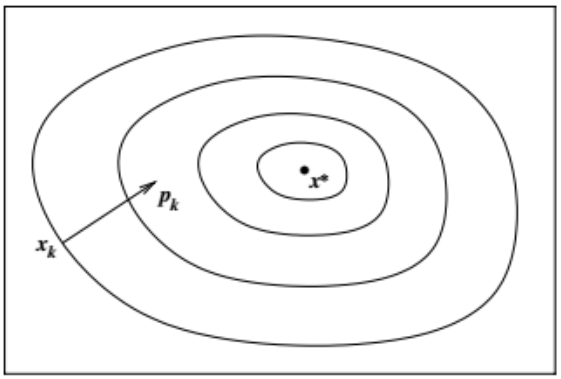

Figure 4.2: Steepest descend direction for a function of two variables (reprinted with permission from Nocedal et al. 2006)

for some $t \in (0, \nabla)$. The coefficient of $alpha$, $p^T \nabla J_k$, is, then, the rate of chance in J along the direction p at x_k. Therefore, the unit direction is given by the minimum value of $p^T \nabla J_k$. Since, $p^T \nabla J_k = ||p||\ ||\nabla J_k||\ cos(\theta)$, the minimum value is when $cos(\theta) = -1$. Finally, one reaches that:

$$p = -\frac{\nabla J_k}{||\nabla J_k||} \tag{4.4}$$

Such direction is orthogonal to the contours of the objective function, as shown in fig. 4.2.

4.3.2 Nonlinear Conjugate Gradient

Nonlinear conjugate gradient algorithm (NLCG) is an adaptation of the conjugate gradient method develop for solving linear equations in the form $Ax = b$, where A is symmetric and positive definite. Such linear case is equivalent to the problem of minimizing the convex quadratic function ($\Phi(x) = \frac{1}{2}x^T Ax - b^T x$). This method takes advantage of the conjugacy property of a set of vector, i.e., a set of nonzero vector $[p_o, p_1, ..., p_n]$ is conjugate with respect to the symmetric positive definite matrix A

if the following equality holds:

$$p_i^T A p_j = 0, \quad for\ all\ i \neq j. \tag{4.5}$$

Recalling eq. (4.4), the search of direction for NLCG algorithm will take the form:

$$p_k = -\nabla J(x_k) + \beta_k p_{k-1} \tag{4.6}$$

where β_k is a scalar that ensures that p_k and p_{k-1} are conjugate. The algorithm, then, takes form of the flowchart in fig. 4.3 as proposed by Fletcher and Reeves.

4.3.3 Selection of Optimization Algorithm

Both algorithms were tested in this thesis with no apparent difference in the final result. However, following a recommendation from *Eclipse Technical Description* (Schlumberger 2014b), which says that the "conjugate gradient algorithm does appear to give a more stable convergence path", we decided to use the NLCG in this thesis.

4.4 Gradient Calculation

In both algorithm discussed in the previous section the critical part is the calculation of the objective gradient function ∇J, which is the sensitivities values of the objective function with regard to the parameters that are allowed to change. For the specific case of reservoir simulation, the objective function depends on both simulation primary variables, X, that is oil pressure, water and gas saturations; and the control parameters, u, which will be defined as the opening set for the ICVs valves. to do this end, we can write the general version of the objective function as:

$$J = J(X(u), u)) \tag{4.7}$$

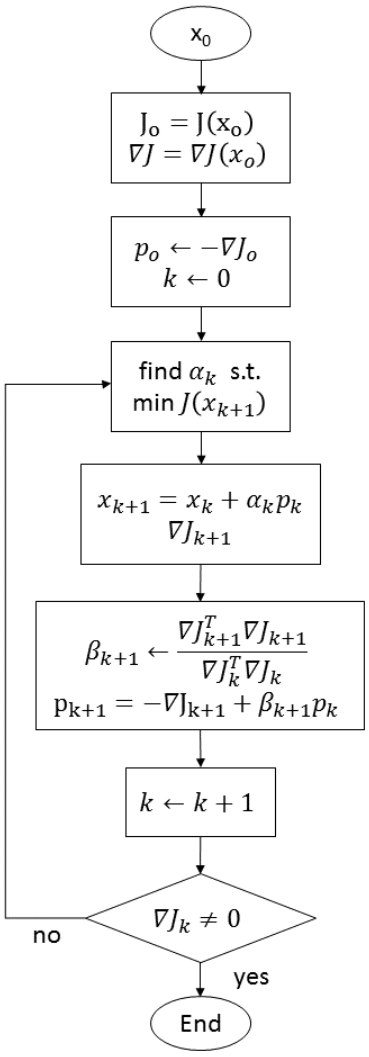

Figure 4.3: Flowchart of the nonlinear conjugate method

The direct approach to calculate the gradient for an specif control parameter, i, can be shown by the total derivative of eq. (4.7) with respect of the control parameter u_i:

$$\frac{dJ}{du_i} = (\nabla_X J)^T \frac{\partial X}{\partial u_i} \tag{4.8}$$

To calculated $\nabla_X J$ one need to recall the reservoir simulations residual equation,

as in eq. (3.78), in the form of $R(X,u)=0$. Then, differentiating it, we have:

$$\left(\nabla_x R^T\right)^T \frac{\partial X}{\partial u_i} + \left(\nabla_u R^T\right)^T \frac{\partial u}{\partial u_i} = 0 \tag{4.9}$$

Rearranging, the following equation is obtained:

$$\left(\nabla_x R^T\right)^T \frac{\partial X}{\partial u_i} = -\left(\nabla_u R^T\right)^T \frac{\partial u}{\partial u_i} \tag{4.10}$$

where the u is the set of all control variables and u_i is an specific one. Therefore eq. (4.10) has as many right-hand sides as parameters, i.e, the direct approach requires one backsubstitution for every control variable, which make this method not attractive for problems with several control variables. This is one of the reason why an adjoint formulation is utilized in the software since in such formulation the effort of calculation is independent of the type or number of control variables.

4.4.1 Adjoint Method

The starting point is the augmented Lagrangian function, L, in which the equality constrain (the reservoir residual equation - eq. (3.78)) is included by multiplying a vector of Lagrange multipliers, λ. Such values can be interpreted as an indication of the cost of a respective constraint, since a value of zero indicates that a respective constraint does not affect the value of the objective function, while a larger number indicates a strong effect.

$$L(X(u),u) = J(X(u),u) + \lambda^T R(X(u),u) \tag{4.11}$$

Since the residual should be equal to zero, $R=0$, the Lagrangian is equal to objective function. Then, taking the total derivative with respect to the control parameters,

u, and suppressing the dependence notation:

$$dL = (\nabla_X J)^T dX + \lambda^T \left(\nabla_u R^T\right)^T du + \lambda^T \left(\nabla_X R^T\right)^T dX \tag{4.12}$$

Since the residual equation is equal to zero, $R = 0$, the vector of the lagrangian multipliers λ can be chosen in any way. Then, by making:

$$\lambda^T \left(\nabla_X R^T\right)^T = -\left(\nabla_X J\right)^T \tag{4.13}$$

eq. (4.12) in no longer dependent on dX. Equation (4.12) can be rearranged to the classical form of the so-called "adjoint system":

$$\left(\nabla_X R^T\right) \lambda = -\nabla_X J \tag{4.14}$$

Recalling eq. (4.12), the total derivative of the Lagrangian can be written with respect to the control parameter, u_i, that is:

$$\frac{dL}{du_i} = \lambda^T \left(\nabla_u R^T\right)^T \frac{du}{du_i} \tag{4.15}$$

The main advantage of the adjoint method is that eq. (4.14) has only to be solved once for every time step, no matter how many control variables the problem has.

4.4.2 Adjoint Method for Discretized Multi-Phase Flow

The development given in this section is based on the work of Rodrigues (2006). In this case, we can rewrite the discretized residual reservoir simulator equation, eq. (3.79), in the following format:

$$r^n = r(x^\nu, x^{\nu-1}, u) = 0, \quad \text{for } n = 1, 2, .., L. \tag{4.16}$$

where L represents the last time step. Next, combining all primary variables from all time steps in one vector X:

$$X = \begin{bmatrix} x^1 & x^2 & \cdots & x^L \end{bmatrix}^T, \tag{4.17}$$

and also combining simulations equation from all time steps in one vetor $R = R(X, u)$:

$$R(X,u) = \begin{bmatrix} r^1(x^1, x^0, u) \\ r^2(x^2, x^1, u) \\ \vdots \\ r^L(x^L, x^{L-1}, u) \end{bmatrix} = 0, \tag{4.18}$$

one can take the total derivative of R to yield:

$$\left(\nabla_X R^T\right)^T dX + \left(\nabla_u R^T\right)^T du = 0 \tag{4.19}$$

Rewriting eq. (4.19) to specify $\frac{dX}{du}$, it follows:

$$\frac{dX}{du} = -\left(\nabla_X R^T\right)^{-T} \left(\nabla_u R^T\right)^T \tag{4.20}$$

Recalling the original goal of optimization of an objective function $J(X, u)$, one take the total derivative with respect to the control parameters:

$$\left[\frac{dJ}{du}\right]^T = \left(\nabla_u J\right)^T + \left(\nabla_X J\right)^T \frac{dX}{du} \tag{4.21}$$

Substituting eq. (4.20) into eq. (4.21), one reaches to:

$$\left[\frac{dJ}{du}\right]^T = \left(\nabla_u J\right)^T - \left(\nabla_X J\right)^T \left(\nabla_X R^T\right)^{-T} \left(\nabla_u R^T\right)^T \tag{4.22}$$

Then, defining the Lagrange multiplier, λ, as follows:

$$\lambda^T = -\left(\nabla_X J\right)^T \left(\nabla_X R^T\right)^{-T} \tag{4.23}$$

one finally reaches the adjoint solution equation:

$$\frac{dJ}{du} = \nabla_u J + \left(\nabla_u R^T\right) \lambda \tag{4.24}$$

From eq. (4.23) it is possible to calculate λ by solving:

$$\left(\nabla_X R^T\right) \lambda = -\nabla_X J \tag{4.25}$$

The adjoint system is then achieved by partitioning λ into L column subvectors of length equal to total number of equations solved by the simulator in one time step (=3 times the number of grid block plus the number of wells equation):

$$\lambda = \begin{bmatrix} \lambda^1 & \lambda^2 & \cdots & \lambda^L \end{bmatrix}^T \tag{4.26}$$

Taking the block bi-diagonal format of $\left(\nabla_X R^T\right)$ into consideration.

$$\left(\nabla_X R^T\right)^T = \begin{bmatrix} \left[\nabla_{x^1}\left(r^1\right)^T\right]^T & 0 & 0 & \cdots & 0 \\ \left[\nabla_{x^2}\left(r^1\right)^T\right]^T & \left[\nabla_{x^2}\left(r^2\right)^T\right]^T & 0 & \cdots & 0 \\ 0 & \left[\nabla_{x^2}\left(r^3\right)^T\right]^T & \left[\nabla_{x^3}\left(r^3\right)^T\right]^T & \cdots & 0 \\ \vdots & \vdots & \ddots & \ddots & \vdots \\ 0 & 0 & 0 & \left[\nabla_{x^{L-1}}\left(r^L\right)^T\right]^T & \left[\nabla_{x^L}\left(r^L\right)^T\right]^T \end{bmatrix} \tag{4.27}$$

where the coefficient matrix $\left[\nabla_{x^n}\left(r^n\right)^T\right]^T$ is simply the Jacobian matrix[1], eq. (3.80), evaluated at r^n. Equation (4.25) can be re-write to the adjoint equations system as follows:

$$\left[\nabla_{x^L}(r^l)^T\right]\lambda^L = -\nabla_{x^L} J \tag{4.28}$$

$$\left[\nabla_{x^l}(r^l)^T\right]\lambda^l = -\left[\nabla_{x^l}(r^{l+1})^T\right]\lambda^{l+1} - \nabla_{x^l} J \tag{4.29}$$

which must be solve backward in time for $l = L-1, L-2, ..., 1$. Once the λ vectors are found from eqs. (4.28) to (4.29), the adjoint solution - eq. (4.24) - can be solved to identify the gradient needed for the optimization algorithm.

1. This fact makes the adjoint method particularly easy to attach to a fully implicit finite-difference simulator that uses Newton-Raphson.

5. METHODOLOGY

The general methodology of this thesis was conceived to make a comparisons between optimization techniques and then evaluate the benefits and drawbacks of each one, where the criteria chosen was based in the economic value of the investment. We have created a work flow that accounts for changes in the reservoir simulator automatically and adopted MatLab as the main optimization platform.

5.1 Softwares

All simulations were implement on the commercial simulator software Eclipse Composition - E300. It should be pointed out that CMG softwares IMEX and its extension ISEGWELL were the initial choice for this thesis. However, the more complicate definition of ICVs and and especially their inconsistent results forced us to a adopt the Eclipse framework - see section 3.4.1 about the multisegment wells.

Although the cases studied are classified as blackoil models (as it will be explained in section 5.3), and therefore the software Eclipse E100 - Blackoil - would be a better fit, the E300 software has a special extension for optimization (see chapter 4), which allow us to work around the problem of information not available to the user, such as the Jacobian matrix.

The computational framework is based on a master program created in MatLab (The MathWorks Inc. 2015). This program was coded in such a way that it makes a communication with the simulator Eclipse in a seamlessly way: it can "call" it and read its outputs files automatically. Such a process allows great flexibility and also the possibility of control loops implementation, where any parameter can be changed in the middle of simulation. The main work flow is depicted in fig. 5.1.

Regarding the restart part of the flowchart in fig. 5.1, two methods are possible:

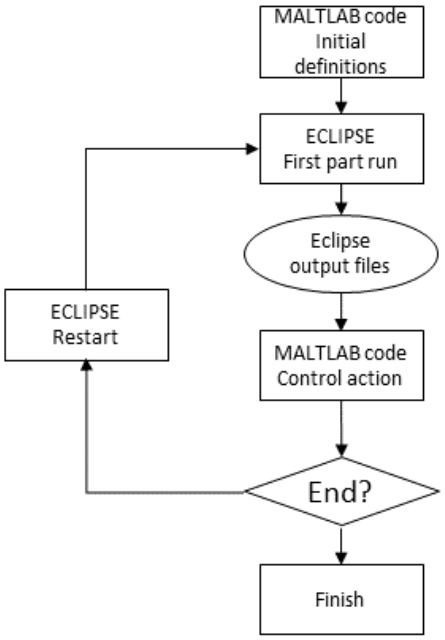

Figure 5.1: Control loop control software implementation

"Fast restart" and "Flexible restart" (Schlumberger 2014b). The former supposed to be the fastest because transmissibilities do not have to be recalculated, meanwhile in the latter method the data must be processed again. However, after intensives tests, the fast restart method showed inconsistent results in cases of several restarts. Furthermore, only the flexible restart method allows the uses of parallel computing. In conclusion, the flexible restart method was chosen in this project.

Nevertheless, it is important to keep in mind that the computation time needed to perform the Flexible restart method increases considerable. A simulation of 120 time steps that would take about 3 minutes in a single run, can take 45 minutes if the restarting in every month. This time can be reduced if the restart time steps is increased, for instance, if restarting every 12 months, the total simulation run takes about 10 minutes.

5.2 Economic Decision

Among several investment yardsticks available such as Finding & Development Costs and Internal Rate of return (IRR), the Net Present Value (NPV) was chosen (Mian 2011). The NPV is a measure of profit created by any investment. The main advantage of this yardstick is that it is a very intuitive and uniform comparison tool: the higher the NPV, the better is the project among mutually exclusive investments opportunities.

The main drawback of the NPV, though, is that its calculation requires the application of a discount factor over the cash flow period, which represents the time value of the money. Since such value is extremely difficult to foreseen in long term projects, in this thesis an nominal discount factor of 10% (ten percent) per year was defined for the sake of simplicity.

Another difficulty, which is shared by all economic yardsticks, is the price foresight. Commodities prices, as explained in section 1.1, are almost impossible to foresee, therefore the recommend method would be the use of stochastic approach. To this end, the decision criteria would be the expected monetary value (EMV) of the NPV. The EMV represents a weighted average of the possible NPV and it is calculated by the following formula:

$$EMV = E\{NPV\} = \sum_{i=1}^{n} NPV_i \times p(NPV)_i$$

where $p(NPV)_i$ is the probability of any specific NPV to happen. Again, such probability is difficult to measure, because it involves both geological and economic uncertainties. Therefore, for the sake of simplicity, the prices were considered fixed over the time period of our simulation.

5.2.1 NPV Calculation

The first step in the NPV calculation is to compute the net revenue of the investment which goes into the calculation of the cash flow. The cash flow represents the total amount of money being transferred into and out of the businesses. Therefore, it can be approximated by the multiplication of the each individual hydrocarbon production (oil and gas) times its relative price discounted by a production tax (representing any Ad Valorem tax, Severance tax and other) minus the respective cost to produces over the time (eq. (5.1)).

$$Net\ Revenue_i = Production_i \times [Prices_i \times (1 - Tax) \times nri - Cost_i \times wi] - (Fixed\ Costs) \times wi \quad (5.1)$$

for $i = 0, 1, ...n$, that is, the every discretized time of the project, and Production, Prices and Cost are defined as follows:

$$Production = \begin{bmatrix} \text{Oil Produced} & \text{Gas Produced} & \text{Water Produced} & \text{Water Injeted} \end{bmatrix} \quad (5.2)$$

$$Prices = \begin{bmatrix} \text{Oil price} & \text{Gas price} & 0 & 0 \end{bmatrix}^T \quad (5.3)$$

$$Cost = \begin{bmatrix} \text{Oil production cost} \\ \text{Gas production cost} \\ \text{Water production cost} \\ \text{Water injection cost} \end{bmatrix} \quad (5.4)$$

There are also two addition terms related to the investment ownership in eq. (5.1): Working (operating) Interests (WI) and Net-Revenue Interest (NRI). The former is a

percentage of the company in the lease contract and shows how much of the cost will be paid by the investor. The latter, on the other hand, measures the percent of profits earned by investor. The NRI is calculated by reducing the revenue obtained by the by all non-operating working interests, such as Royalties (i.e. production retained by mineral interest owner - individuals or governments - when lease is obtained), as shown in eq. (5.5).

$$nri = (1 - royalty) \times wi \tag{5.5}$$

The cash flow, then, is obtained by taking the the Capital Expenditures (the initial investments such drilling) and the Abandonment cost (cost related with environmentally safe abandonment of wells and facilities at end of economic life of project) into consideration:

$$CASH\ FLOW = Net\ Revenue - CAPEX - (Abandonment\ Costs) * wi \tag{5.6}$$

Finally, the NPV is calculated by the summation of the cash flow over time discounted by the time value of money:

$$NPV = \sum_{n=0}^{N} \frac{CASH\ FLOW}{(1-i)^n} \tag{5.7}$$

where i is the discounted factor, n is a specific time and N the end of economic life of project.

For the sake of simplicity, no after tax cash flow was considered in this thesis. That is, neither depreciation, depletion, and amortization nor federal income tax were include in economic evaluations, as well as, no inflation was take into consideration.

5.2.2 End of Economic Life of Project

All simulations in Eclipse were specified to run for a predefined period time, for instance 20 years. However the end of economic life of project in the vast majority of cases were lower than this period. The method to identify this time was to check when the cash flow becomes negative. When this happens, there is no logic to continue operations since the investor is actually losing money, so every result after this point is simply ignored. The sketch in fig. 5.2 shows this methodology.

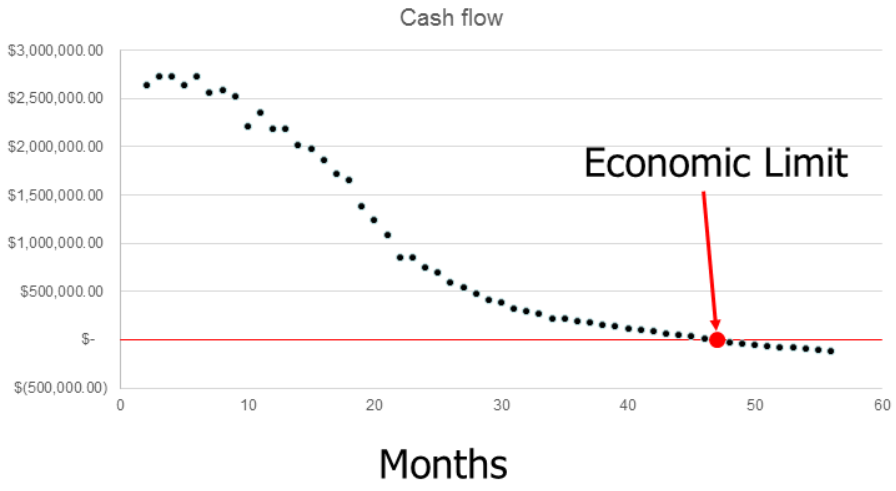

Figure 5.2: End of economic of a project

5.3 Overall Approach

In order to make a fair comparison between conventional and "smart" waterflooding, four different strategies were tested throughout this theses. The first two are based in convention well completion wells while the last two are equipped with ICVs but with different types of control. They are as follows:

I - Base case - Fully open: In this case, any potentially well is fully completed in all

layers. The simulation runs until the economic limit is reached. This case will be used as the base case for comparison purposes.

II - Optimal completions: In this case, tests are performed well-by-well by trial-and-error to find what would be the best configuration completion. For instance, considering a reservoir with 10 layers, all 1023 possible combinations are tested. This test gives insights about layers with possible high permeability channels that causes an early breakdown compromising the entire well, and therefore may not be open for production.

III - Variable control: A reactive variable control (based on Dilib et al. 2013; Dilib et al. 2015) was realized to test the claim that simple control techniques would do a better work for reservoir subject to major geological uncertainties. More about this strategy will be explained in section 5.4.

IV - Optimal control: Based in the optimization algorithms explained in chapter 4, a model-based gradient optimization was implement. The goal here is to try to identify the maximum economic potential of the reservoir.

All previous strategies are based in a deterministic approach, which means that we assume perfect knowledge of the reservoir. However, all reservoir properties contains relative uncertainties at some level . Therefore, unless the reservoir characterization is very accurate (which may no be practical in many realistic reservoirs due to sparse measurements), such strategies will probably not give the full picture of the potential

differences between different realizations of the porous media. An attempt to overcome this problem is to try different reservoir realizations hoping that this captures all possible reservoir behaviors. Because of this, an extra test was designed:

V - Robustness check: In this test, the same strategies of the previous tests are employed again, but in different reservoir realizations. Where, for the sake of simplicity, only the permeability field is altered, keeping other properties, such as porosity, unchanged. Important to say that any eventual parameter tunned in the previous strategies was kept unchanged for this test. The idea is that one realization is the most probable one and the others, possibles ones with less probability to happen.

5.4 Variable Control

The works of Dilib et al. (2013) and Dilib et al. (2015)[1] suggests that simple direct feedback control between reservoir monitoring and ICV settings could yield to reasonable results. Such a strategy consists in monitoring well and completions water-cuts and, then, design the percentage of the closure of the ICV.

Following the flowchart of fig. 5.3, initially all ICV are set to operate fully opened. Then, if the wellhead water-cut W_w exceeds a predefined trigger W_t, the algorithm goes to the next step. If the algorithm is triggered, the water-cut respective to every valve in the well (see fig. 3.4) is checked. The valve with the minimum vale of water-cut is then set to completely open, and the other are choke using the following equation

$$u_i\% = max\left[1 - \left(\frac{W_i - W_m}{W_l - W_m}\right)^c, 0\right] \tag{5.8}$$

1. Their model was a sandstone reservoir with interbedded shales and a aquifer with only one horizontal well with two ICVs, one in the toe and other in the heel.

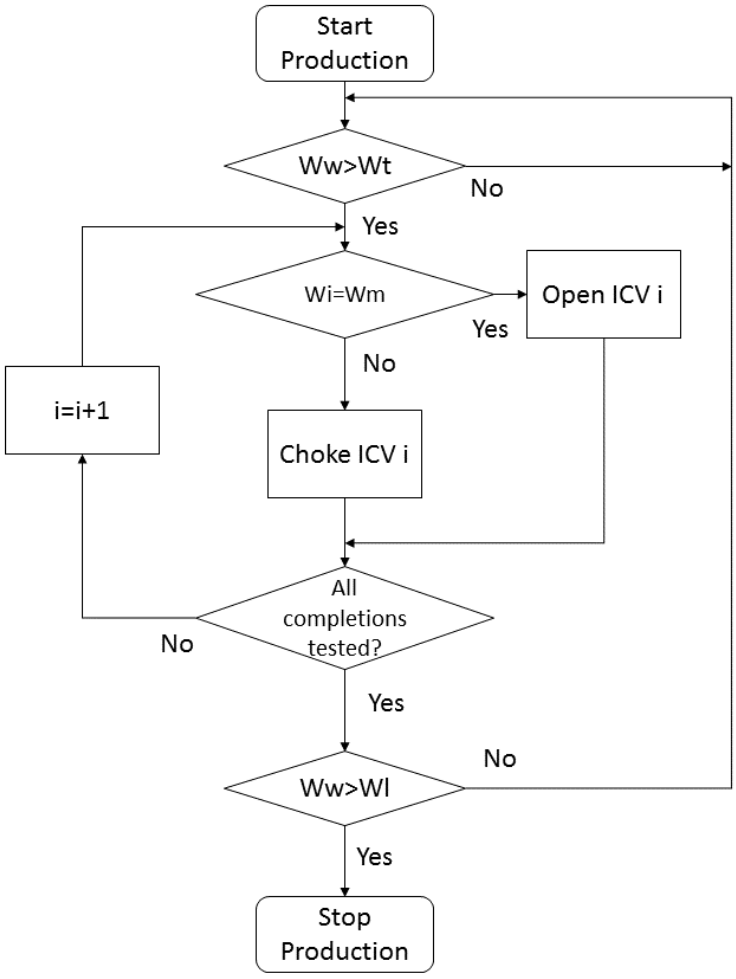

Figure 5.3: Flowchart of the variable control (adapted from Dilib et al. 2013)

where $u_i\% \in [0, 1]$ is the opening set of the valve, W_i is the water-cut relative to the ICV_i, W_m is the minimum water-cut measured between all ICVs, W_l is the maximum well water-cut limit, and c is an exponent of proportionality. This equation is basically the negative of a simple proportionality: the bigger the water-cut, the more closure the ICV should have.

Due to fact that the ICV is modeled as a function of the range in the openning of the valve (see section 3.4), the $u\%_i$ must be scaled to the minimum and maximum

valve opening to honor respectively eqs. (3.89) and (3.90), so:

$$u_i = u\%_i(A_{c_{max}} - A_{c_{min}}) + A_{c_{min}} \tag{5.9}$$

Finally, the last check is to see if the well water-cut is bigger the the maximum well water-cut allowed, W_l. If so, the well is closed.

5.4.1 Variable Control Parameters Tuning

The variable control has then three parameters to chose: W_l, c, and W_t. In addition, two parameters were included in the original formulation: δt, the lagging time between actions and "re-open action", e.g. the ability or not to reopen one valve once closed. The lagging time is an attempt to compensate the slow dynamics of the reservoir system since the measurement and action point are in the same physical instrument. It is the minimum time one action (close or open valves) is allowed after a previous action. So, four lagging time were tested: 1 month, 3 months, 6 months and 1 year.

The "reaction time" tries, on the other hand, to avoid one possible problem with the ICV control based on water-cut measurement. At the grid block level, one does not have a direct way to decrease the quantity of water, because the water is always being pumpep in the injectors water and there is no source of pressure that affects only the oil phase. Therefore, the ICV most probably will behave as an on/off control, closing and opening at sequentially times[2].

These five parameters, then, were chosen by a complete search to certain arbitrary parameters. With the exemption of W_t, which was set to 1%, for the sake of

2. Because of this two problems (measuremente and action in the same point, and no direct control to decrease the water-cut), the original idea for this thesis research had to be interrupted. It was based in using control techniques from control and automation engineering that could be applied to the spatial linearized reservoir equation - eq. (3.58).

simplicity. The values tested were then:

- Wl was allowed to be 50%, 80%, or 90%.
- c was allowed to be 1, 2, 3 or 4.
- δt was allowed to be 1 month, 3 months, 6 months and 1 year.
- "re-open action" was allowed to be "yes" or "no".

this makes a total of 95 simulations in which the parameters were set according to the one with the big NPV. It should be pointed out that, all this tests were performed only with the most probable realization; so, they were all kept unchanged in the robustness check.

6. CASE STUDIES

Two type of reservoir models were studied in this thesis, being one very simple and the second more complex wih multiples realizations. The first one, that will be describe in section 6.1, is a synthetically cube with a five-spot waterflooding configuration. The second reservoir model is a more complex with more wells, which will be fully described in section 6.2.

6.1 Simple Model

This model, inspired on Pinto (2013), has one producing well in the center and 4 water injectors at corners. The aim of this simple reservoir is not only to test all programming code, but also to analyze more simple configurations.

Generally speaking, it could be interpreted as a section of a much bigger reservoir. The reservoir has dimension of 41x41x10 grid blocks, with one grid block having dimensions of 20x20x10 meters, respectively. The rock and water properties have been listed in table 6.1. This reservoir properties are based on Pinto 2013.

Table 6.1: Simple model - rock and water properties

Parameter	**Value**	**Units**
Reference pressure of the rock	315.56	bar
Rock compressibility	5.41×10^{-5}	bar^{-1}
Reference pressure of the water	0.98	bar
Water compressibility	4.9966×10^{-5}	bar^{-1}
Water density	1.01	-

The permeability and the porosity fields have been constructed using probabilistic distribution in attempt to give more realism to the system. The permeabilities fields

Table 6.2: Simple model - permeability and porosity distribution

Parameter	**Values**
X permeabilities (layers 1, 5, and 9)	ln $\mathcal{N}$ (μ=600 md, σ^2=200^2 md^2)
X permeabilities (layers 3, and 7)	ln $\mathcal{N}$ (μ=300 md, σ^2=100^2 md^2)
X permeabilities (layers 2, 4, 6, 8, and 10)	ln $\mathcal{N}$ (μ=150 md, σ^2=50^2 md^2)
Y permeabilities	Equal to X permeabilities
Z permeabilities	10% of X permeability values
Porosity	$\mathcal{N}$ (μ=0.15, σ^2=0.05^2)

were generated by log-normal distribution - ln $\mathcal{N}(\mu, \sigma^2)$ - with different values for each layer; and the porosity field, by a normal distribution - $\mathcal{N}(\mu, \sigma^2)$. Table 6.2 lists such values and fig. 6.1 shows the Petrel screen shot of the reservoir with the five-spot configuration.

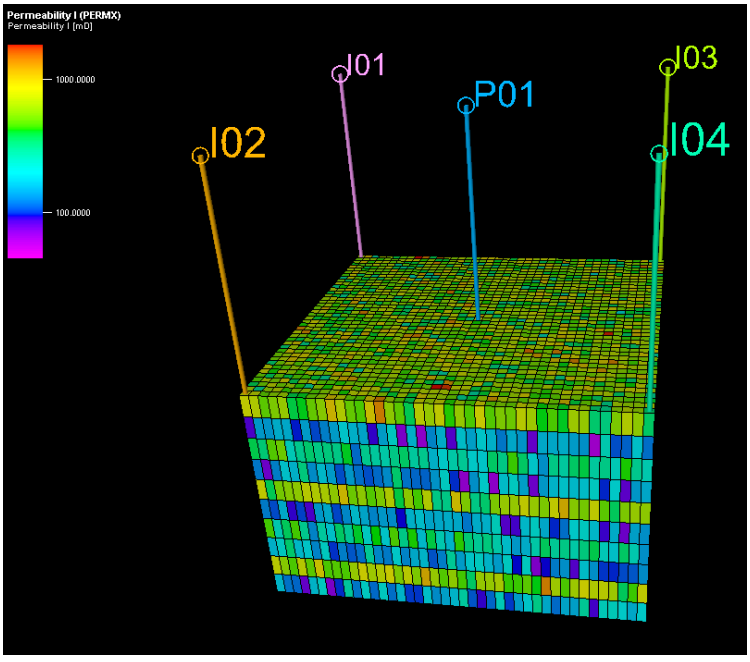

Figure 6.1: Simple model - reservoir field with wells

Regarding the fluid properties, this model uses a light oil (API 31.9°) with characteristics of the Namorado field, offshore Brazil. The bubble-point pressure is 3,045.8 psi (210 bars) and the initial pressure is 4568.7 psi (315 bars). Figure 6.2 shows the viscosity (μ) and oil formation volume factor (B_o) curves. While fig. 6.3 shows the water and oil relative permeabilities curves.

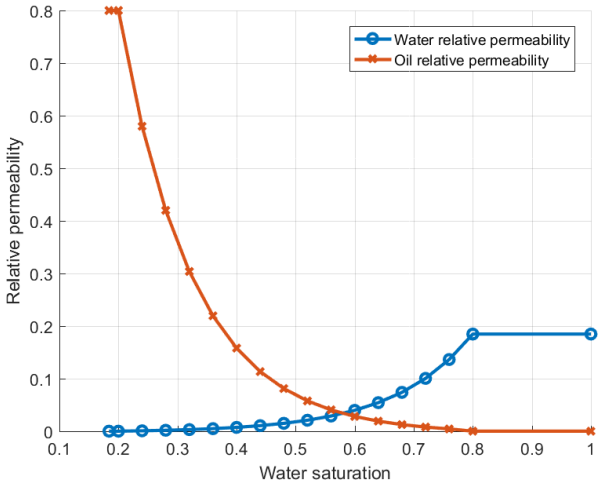

Figure 6.2: Simple model - viscosity and oil formation volume factor

6.1.1 Well Operation

The model has 5 verticals wells: one producer at center and 4 injector at the corners. Their operation conditions are specified in table 6.3. Such parameters are constant over all simulation time.

The total water volume injection rate for all injectors is also controlled by voidage replacement system, where the total injection rate is equal to the total production voidage rate.

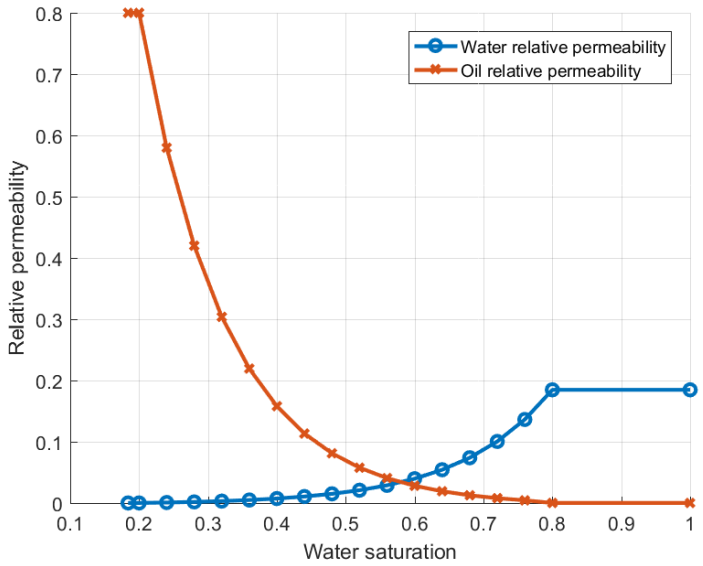

Figure 6.3: Simple model - water and oil relative permeability

Table 6.3: Simple model - well operation constraints

Producer well		**Injector wells**	
Max flow rate	15,725 STB/day	**Surface max flow rate**	10,065 STB/day
Minimum BHP	2,900 psi	**Max BHP**	5,800 psi

6.1.2 Economic Parameters

In order to perform the calculation of the NPV, commodities prices and production costs must be input in the code. As already explained in section 5.2, the prices were kept constants throughout the simulation time. Interesting to note that "Disposal Water" represents the cost to handle the produced water, since such water requires a specific treatment.

In addition to the production related cost, there are the capital expenditures, which, for the sake of simplicity, were summarized in table 6.5. Therefore, since this model has 5 wells, the total CAPEX will be $10,000,000.00; the abandonment cost,

Table 6.4: Selling prices and production costs

Selling prices		**Production costs**			
Oil	**Gas**	**Oil**	**Gas**	**Disposal Water**	**Injection water**
$ 30.00/bbl	$ 3.00/MMbtu	$ 8.00/bbl	$ 0.20/MMbtu	$ 1.70/bbl	$ 1.00/bbl

$250,000.00; and the fixed costs, $7,500.00 per month.

For the intelligent wells, there is an extra cost of $200,000.00 per well, plus $200,000.00 for every additional ICV (Pinto et al. 2015). So, for instance, a well with 3 ICVs will cost $600,000.00 more if compared to an conventional well.

Table 6.5: Capital expenditures and fixed cost

CAPEX	$2,000,000/well
Abandonment:	$50,000/well
Fixed cost	$1,500/well/month
Intelligent completion	$ 200,000.00
Additional ICV	$ 200,000.00

Finally, the last definition for the NPV calculation is related to ownership of the reservoir. There can be a distinction of values "before payout" (BPO) and "after payout" (APO), however this was not the case is this thesis and both values were kept the same. Then, according to eq. (5.5), Net-Revenue Interest (NRI) is 87.5% .

Table 6.6: Ownership distribution

	BPO	**APO**
Working Interest	100.00%	100.00%
Royalty:	17.50%	17.50%

6.1.3 Base Case and Optimal Completion Results

Following the methodology of chapter 5, all different types of completions were tested to identify the configuration that would optimize the financial return. So, for this case, since there are 10 vertical layers along the well direction, the number of test was found by the total number of possible combinations:

$$N_{test} = \frac{10!}{(10-1)!1!} + \frac{10!}{(10-2)!2!} + \frac{10!}{(10-3)!3!} + \frac{10!}{(10-4)!4!} + \frac{10!}{(10-5)!5!} + \frac{10!}{(10-6)!6!} + \frac{10!}{(10-7)!7!} + \frac{10!}{(10-8)!8!} + \frac{10!}{(10-9)!9!} + \frac{10!}{(10-10)!10!} \quad (6.1)$$

plus one more case, which is the base case where all completions were set open, totalizing 1,024 tests. Table 6.7 summarize the ten best results plus the base case. Its 7 columns represents, respectively: the ranking of the configuration among all test, the NPV achieved, the end of economic life of the project, the amount of oil produced, the amount of gas produced, the amount of water produced, and, finally, the amount of water injected.

Table 6.7: Simple model - summary of the 10 best results and basecase

Ranking	**NPV**	**Economic Limit (months)**	**FOPT (bbl)**	**FGPT (scf)**	**FWPT (bbl)**	**FWIT (bbl)**
1	$ 86,430,383.92	62	3.233E+6	353.614E+6	430.984E+3	4.765E+6
2	$ 86,427,816.86	68	3.184E+6	348.264E+6	302.048E+3	4.570E+6
3	$ 86,385,045.26	71	3.167E+6	346.400E+6	263.070E+3	4.509E+6
4	$ 86,369,639.53	68	3.190E+6	348.930E+6	324.482E+3	4.601E+6
5	$ 86,366,108.85	66	3.212E+6	351.274E+6	367.170E+3	4.672E+6
6	$ 86,346,321.00	60	3.248E+6	355.196E+6	496.565E+3	4.850E+6
7	$ 86,340,982.81	56	3.273E+6	357.942E+6	592.498E+3	4.980E+6
8	$ 86,335,078.86	60	3.247E+6	355.165E+6	495.550E+3	4.848E+6
9	$ 86,334,777.99	68	3.183E+6	348.081E+6	305.531E+3	4.572E+6
10	$ 86,326,798.64	62	3.237E+6	353.992E+6	451.602E+3	4.790E+6
558	$ 85,467,828.50	46	3.143E+6	343.731E+6	293.524E+3	4.506E+6

The closed completion for these 10 best configurations are shown on table 6.8, where the numbered columns represents then quantity of completions that should be closed, and the number in each cell represents which layer is closed.

Table 6.8: Simple model - closed completions for the 10 best cases

n=1	**n=2**	**n=3**	**n=4**	**n=5**	**n=6**	**n=7**	**n=8**	**n=9**	**n=10**
1	2	3	8	9	0	0	0	0	0
1	2	5	8	9	0	0	0	0	0
1	2	5	6	9	10	0	0	0	0
1	2	5	9	10	0	0	0	0	0
1	2	3	6	8	9	0	0	0	0
1	2	4	8	9	0	0	0	0	0
1	2	8	9	0	0	0	0	0	0
1	2	6	8	9	0	0	0	0	0
1	4	5	8	9	0	0	0	0	0
1	2	3	9	10	0	0	0	0	0

Number and position of the ICVs

From table 6.8, an engineering and practical approach was defined to find the number and allocations of the ICV necessary for the next production strategy used in the variable control. Taking the very best configuration, one note that the layers 1, 2, 3, 8, and 9, are kept closed for the whole project time. The claim here, then, is that these layers can produce some hydrocarbons before this layer face a water breakthrough.

So, following the multisegment representation (section 3.4.1), the ICV were allocated according fig. 6.4. Note that, since there is no valve allocated to branches 2 and 4, the corresponding layers are free to produce all over the time and there is no method to prevent them to produce only water.

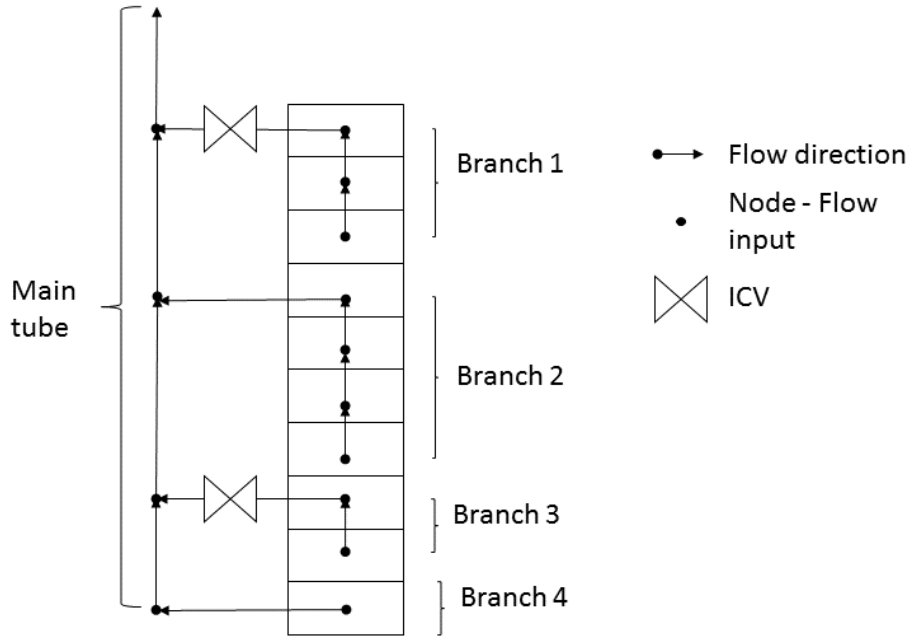

Figure 6.4: Simple model - multisegment configuration

6.1.4 Variable Control

The variable control, as explained in section 5.4, has 4 parameters fo tuning. One strategy to do this would be to perform an optimization algorithm. However, such approach goes against the assumptions of improve production without fully knowledge of the reservoir model. Another strategy would be to perform a robust optimization, that is, perform an optimization for every possible and imaginable reservoir model and then take the the parameters that gives the best expected value of mean. The drawback for such strategy is the computation time, for instance, if there are 100 possible models, every single simulation with a monthly restarting time takes 45 minutes, and for every model a optimization algorithm would need at least a couple simulations. So, the computation time is practically restrictive.

Therefore, a more pragmatic strategy was adopted. From section 5.4.1, some

values for the 4 control parameters were allowed. Then, a complete search is executed, that is, of possible combinations are tested. Finally, the control parameters are chosen from the simulation that presents the best NPV.

Table 6.9 summarizes the best 10 results obtained. The columns of such table have the following meaning, respectively: order ranking; the well water-cut limit; if re-open a closed ICV is allowed or not, zero means "no" and 1, "yes"; δ_t is the lagging time between actions; "c" is the proportional exponent of eq. (5.8); "Economic limit" represents the end of life of the project in months; "total investments" is the sum of all expenditures made to start the production plus the cost of intelligent completions and ICVs; the last 4 columns are respectively: the oil, gas, water productions and the total water injected.

In conclusion, the best parameter for the variable control are: δ_t is equal to 1 (i.e. the control algorithm measure and acts every months), the proportional exponent is equal to two, the maximum well water-cut is equal to 90%, and, finally, no reopen is allowed (i.e. this avoids the unceasingly effect on-off).

6.1.5 Optimal Control

To compare this result with a possible "optimal" production that the reservoir can offer, the nonlinear conjugate algorithm with adjoint formulation was applied (chapter 4). The mathematical formulation is according to equation

$$\begin{aligned} \max_{u\in[0,1]} \quad & NPV(u) \\ \text{subject to} \quad & R(u) = 0 \end{aligned} \tag{6.2}$$

where R is the residual reservoir equation - eq. (3.78) - and u is a vector with all valves closing set position in all times. So, for this specific case, with the simulation time of 10 years (this is not the end of project life, which could be less according

Table 6.9: Simple model - variable tunning search results

Ranking	W_l	**Alternate?**	δ_t	**c**	**NPV**	**Economic Limit (months)**	**Total Investment**	**FOPT (bbl)**	**FGPT (scf)**	**FWPT (bbl)**	**FWIT (bbl)**
1	90	0	1	2	$ 85,742,065.50	62	-$ 11,850 million	3.17E+6	347.06E+6	288.26E+3	4.54E+6
2	90	0	1	1	$ 85,719,849.31	63	-$ 11,850 million	3.17E+6	347.02E+6	282.44E+3	4.54E+6
3	90	0	3	2	$ 85,667,649.41	60	-$ 11,850 million	3.17E+6	346.88E+6	292.42E+3	4.55E+6
4	90	0	6	1	$ 85,667,460.30	60	-$ 11,850 million	3.17E+6	346.88E+6	292.41E+3	4.55E+6
5	90	0	6	2	$ 85,667,448.83	60	-$ 11,850 million	3.17E+6	346.88E+6	292.41E+3	4.55E+6
6	90	0	3	1	$ 85,658,513.55	63	-$ 11,850 million	3.18E+6	347.33E+6	293.56E+3	4.56E+6
7	90	0	1	3	$ 85,650,430.26	58	-$ 11,850 million	3.17E+6	346.74E+6	292.84E+3	4.54E+6
8	90	0	1	4	$ 85,615,798.20	57	-$ 11,850 million	3.17E+6	346.80E+6	297.33E+3	4.55E+6
9	90	0	3	3	$ 85,567,948.83	56	-$ 11,850 million	3.17E+6	346.48E+6	293.93E+3	4.54E+6
10	90	0	3	4	$ 85,567,862.97	56	-$ 11,850 million	3.17E+6	346.48E+6	293.95E+3	4.54E+6

to a negative cash flow), and with the valves allowed to change every month, the u vector has the dimension of 240 variables (2 valves times 120 months)[1].

It is well known that reservoir simulation problems are large scale nonlinear systems with the additional difficult of large geological uncertainties. Therefore, the local optimization solution is difficult issue to find. The solution is then very dependent on the initial guess and,if it is relatively close to any local solution, the algorithm will most likely be trapped at this points. So three initial guesses were used:

- 1 - The valves setting parameter found by the variable control.
- 2 - All valves opened since the beginning
- 3 - All valves set in mid range position since the beginning.

Table 6.10 summarizes the optimization algorithm results according to the initial guess. Not surprisingly the NPV results were a little better and came from the first type of initial guess.

Table 6.10: Simple model - optimization results

Initial Guess	**NPV**	**Economic Limit (months)**	**FOPT (bbl)**	**FGPT (scf)**	**FWPT (bbl)**	**FWIT (bbl)**
1	$ 86,229,427.70	63	3.17E+6	347.22E+6	289.41E+3	4.55E+6
2	$ 85,407,009.30	52	3.17E+6	346.27E+6	302.65E+3	4.55E+6
3	$ 85,500,277.86	56	3.17E+6	346.33E+6	294.40E+3	4.54E+6

1. The adjoint method is the recommend method to find the gradient because the number of parameters (240) is bigger than the "observed data" (120).

6.1.6 Simple Model Case Conclusion

Table 6.11 compiles the results of the simple model case, where ΔNPV is the absolute difference between the control method in question and the base case and $\Delta NPV\%$ in relative gain $\left(\Delta NPV\% = \frac{\Delta NPV}{NPV_{Basecase}}\right)$. The best results were achieved with the best completions configuration. This is due to the less capital expenditure necessary for this wells, which gives an initial economy of $ 600,000.00 relatively to the intelligent completion and two ICVs.

Table 6.11: Simple model - summary

Case	**NPV**	**ΔNPV**	**ΔNPV%**
No ICV, 10 completions	$85.468E+06	$000.000E+00	0.00%
Optimal completions	$86.430E+06	**$962.555E+03**	**1.13%**
Variable control	$85.742E+06	**$274.237E+03**	**0.32%**
Optimal Adjoint Method	$86.229E+06	**$761.599E+03**	**0.89%**

For easier visualization, table 6.11 was expressed graphically in fig. 6.5. It is clear that although the absolute gain were relative high in all scenarios, the relative gain were low (between 0.2% and 1%). One possible explanation is that the reservoir model was too "homogeneous" in the five-spot configuration, so any eventual gain of using ICVs (e.g. avoid early breakthrough) is masked by the nice flow configuration in the reservoir. For instance, if one layer is closed by an ICV, the pressure energy in this reservoir "push" the water to an adjacent layer.

Because this simple model was intended for programing purposes and initial conclusions, no further test were implemented (robustness check). Also, no further information is expected since the homogeneity of the model jeopardizes gain differences, so it is most probable that test different models will have worse results since

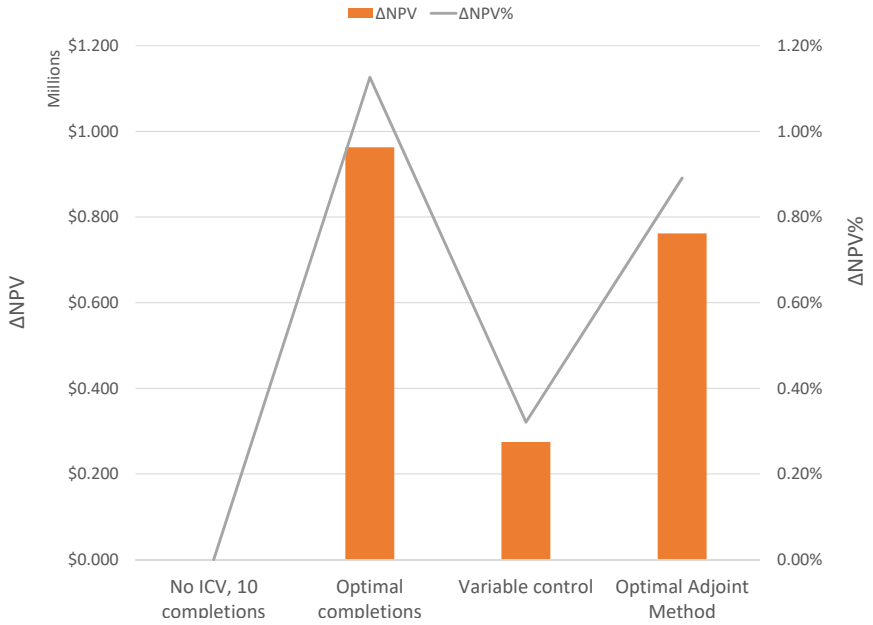

Figure 6.5: Simple model - summary

neither a new tunning nor any optimization algorithm is applied.

6.2 Egg Model by TU Delft

The egg model is a benchmark develop in TU Delft university, The Netherlands (Jansen et al. 2014). It is a synthetic channelized reservoir model that tries to mimic typical meandering river patterns encountered in fluvial environments. It works under water flooding conditions with eight water injectors and four oil producers. Figure 6.6 shows the reservoir configuration.

The benchmark also comes with an ensemble of 100 different three-dimensional realizations, besides the most probable one. Figure 6.7 shows six randomly chosen realization to demonstrate the differences with their clearly channeled orientation. It's important to note that the channels have not been conditioned to always match

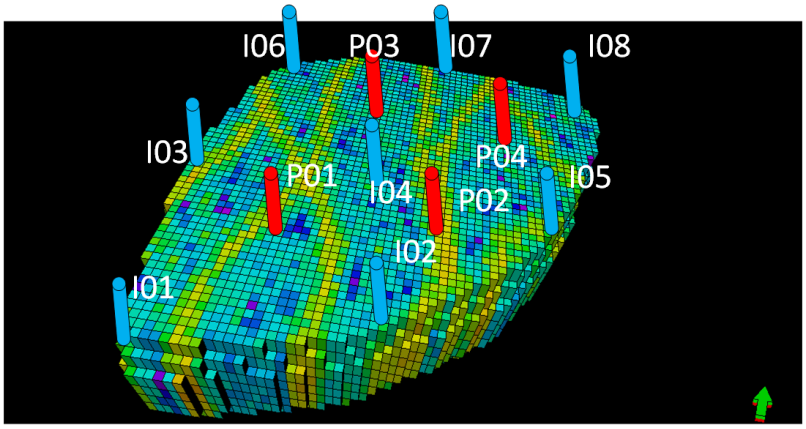

Figure 6.6: Egg model reservoir - most probable one

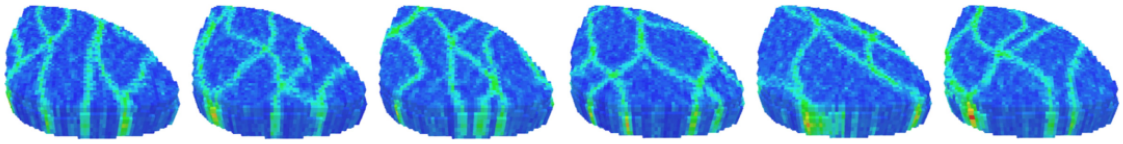

Figure 6.7: Different realizations of the egg model

the wells positions.

The parameters for the standard model are listed in table 6.12 and the relative permeabilities curves are shown in fig. 6.8.

Originally this benchmark was a two phase (oil and water) reservoir with no gas, however, since E300 compositional simulator demands a third phase, a gas phase was include in the dataset. To do this, a "dummy" table was added in such a way that the bubble point was so low compared with the reservoir pressures that no significant gas was produced. This will become clearer from the amount of gas produces in the simulations presented.

Table 6.12: Egg model - reservoir and fluid properties

Parameter	**Values**
Grid-block height, h	13.1 ft
Grid-block length/width, $\Delta x, \Delta y$	26.2 ft
Porosity, ϕ	0.2
Oil compressibility, c_o	6.89x10^{-7} psi^{-1}
Rock compressibility, c_r	0.0 psi^{-1}
Water compressibility, c_w	6.89x10^{-7} psi^{-1}
Oil Dynamic viscosity, μ_o	5.0 cP
Water Dynamic viscosity, μ_w	1.0 cP
End-point relative permeability, oil, Kr_o^0	0.8
End-point relative permeability, water, Kr_w^0	0.8
Corey exponent, oil, η_o	4.0
Corey exponent, water, η_w	3.0
Residual-oil saturation, S_{or}	0.1
Connate-water saturation, S_{wr}	0.2
Capillary pressure, p_c	0.0
Initial reservoir pressure (top layer), p_r^{top}	5,800 psi
Initial water saturation, $S_{w,0}$	0.1
Water injection rates, per well, q_{wi}	500.0 bbl/day
Production well bottom-hole pressure, p_{bh}	5,730.0 psi
Well-bore radius, r_{well}	3.9 inches
Simulation time, T	3600.0 days

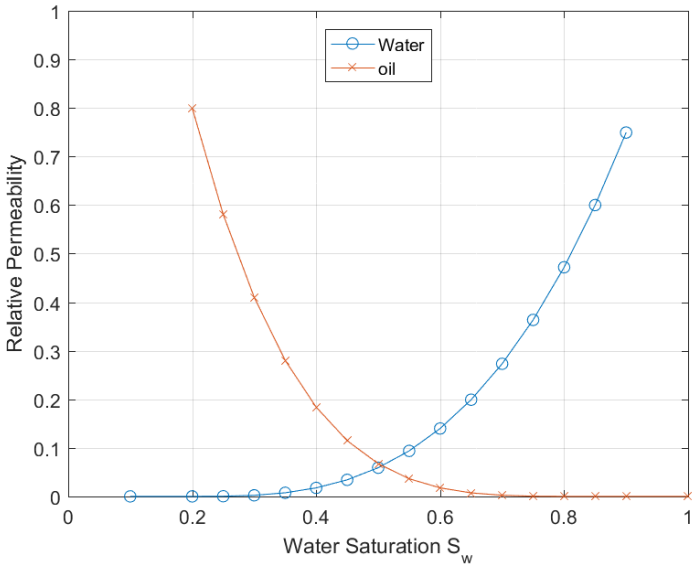

Figure 6.8: Egg model - relatives permeabilities

6.2.1 Economic Parameters

The economics definition for this case are the same as the simple model case, discussed in section 6.1.2. The exception, however, is the oil price, which was increased from $ 30.00 to $ 50.00[2]. Therefore, there is only one table that need to be update (see table 6.13).

Table 6.13: Egg model - selling prices and production costs

Selling prices		**Production costs**			
Oil	**Gas**	**Oil**	**Gas**	**Disposal Water**	**Injection water**
$ 50.00/bbl	$ 3.00/MMbtu	$ 8.00/bbl	$ 0.20/MMbtu	$ 1.70/bbl	$ 1.00/bbl

2. Manly because the real price has reached approximated this level by the time this case had started.

6.2.2 Base Case and Optimal Completion Results

Compared to the simple model case, an additional problem arises here due to the fact that there are four producers wells instead of only one well. So, since each well has 7 layers, there are in total 127 possible combinations. Then, counting all four wells, there are 127^4 combinations, that is, to actually perform a complete search to find the best completion optimization, one would have to do 260,164,641 simulations, which is obliviously impractical.

Following a more pragmatic and practical engineering point of view, the approach adopted here is to individually test each well keeping the other fully opened, which reduces the number of simulations to 509 simulations ($4 \times 127 + 1$ base case). Table 6.14 summarizes the results obtained per well. The columns of such table mean, respectively: (1) the well number, but zero means the base case where all completions of all wells are open; (2) ranking of this configuration amongst the total 509 simulations (note that the 33 first best completions are related with 2); columns (3) to (8) were already defined in previous tables; columns (9) to (15) - "Completions closed" - show which completion were closed per well.

Table 6.14: Egg model - best completions summary per well

Well	**Ranking**	**NPV**	**Economic Limit (months)**	**FOPT (bbl)**	**FGPT (scf)**	**FWPT (bbl)**	**FWIT (bbl)**	**Completions closed**						
2	1	$ 18,299,136.00	39	510.9E+3	957.9E-15	1.8E+6	2.3E+6	2	3	4	5	6	7	0
1	33	$ 15,792,030.02	41	501.7E+3	940.7E-15	1.8E+6	2.3E+6	1	2	3	4	5	6	7
4	205	$ 14,781,648.71	50	499.9E+3	937.4E-15	1.8E+6	2.3E+6	1	2	3	4	5	6	7
0	257	$ 14,471,401.53	45	426.2E+3	799.1E-15	444.4E+3	870.7E+3	0	0	0	0	0	0	0
3	259	$ 14,419,954.14	45	498.0E+3	933.8E-15	1.8E+6	2.3E+6	6	0	0	0	0	0	0

So, analyzing well 2, the best configuration would be closing layers 2 to 7, and leaving layer 1 opened. Interestingly, wells 1 and 4 should be kept always closed.

Regarding well 3, even the best configuration is ranked below the base case. It should be emphasized that such conclusions relies in separate and individual analysis, not taking the interference between wells in consideration and, thus, care must be taken for find analysis.

Number and position of the ICVs

This is probable the more complex and difficult decision that must be made when intelligent completions are considered. An optimization to identify the "best" location was discarded because the whole point of the introduction of ICVs is the partial knowledge of the reservoir model. Another possible criteria would be to put the valves in the high permeability layers, but that would work only for layered reservoirs, in which the permeability is homogeneous in each layer. Finally, the criteria adopted is based on the results from table 6.14, where wells 1 and 4 have all of its layers closed in the best cases, and well 2 have only one layer opened.

The next difficult questions to answer are how many ICVs per well and in which layers to allocate them. First, the number of valve was defined by taking into account the relative price against the total NPV in the base case scenario. So, for instance, a total of 6 ICV s would cost $ 1,800,000.00, which represents approximately 12% of the base case NPV $\left(\frac{1,800,000}{14,471,401.5}\right)$. The allocation question was answer by trying to split each well in two independent sections. Because there is an odd number of layers (7), there was a little preference for the upper layers since the oil density is smaller than the water.

Finally, the multisegment representation of wells 1, 2, and 4 was made according to fig. 6.9. Since any different configuration in well 3 jeopardizes the production when compared with the bases case, this well was left completely open.

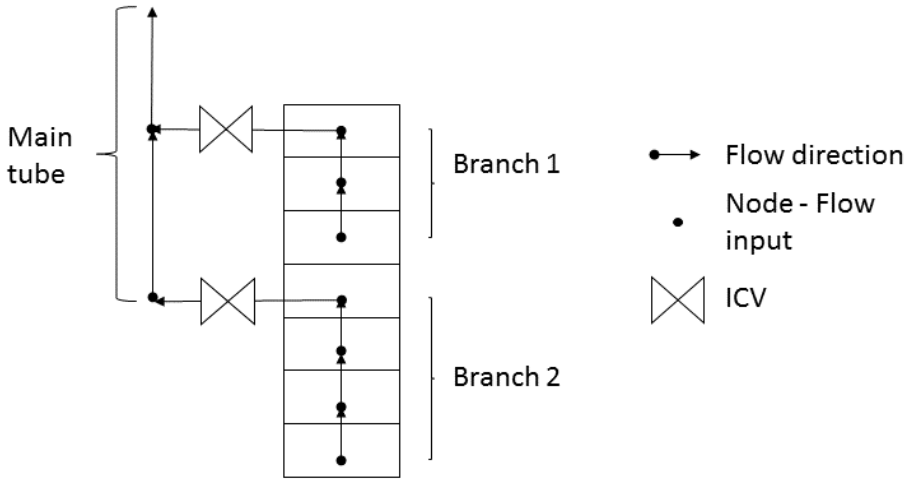

Figure 6.9: Egg model - multisegment representation for wells 1, 2, and 4

6.2.3 Variable Control

As in the simple model case (section 6.1.4), the same pragmatic complete search in the variable parameters was made. Table 6.15 summarizes the best 14 results. Interestingly, the best case was when the lagging time, δ_t, was 12 months (that is, after an action in any valve, the next allowed action was only one year latter), and maximum well water cut of only 50% (a very low level). These counter-intuitive results are indicatives of the very complex, but also slow flow dynamics in a reservoir simulation with multiples wells and complex permeability field.

Another interesting point comes from the "re-open" capability, which rank several case amongst the best, including the very best case. For the case when δ_t is 12 months, an explanation could be the long lagging time period, that is, there is sufficient time for water to move through pressure differential to other parts of the reservoir. However, for the case where δ_t equals to 1 (seventh ranking position), it is difficult to find a physical explanation. Again, this counter-intuitive result reinforce the idea that we are dealing with very complex dynamics in the reservoir.

Table 6.15: Egg model - variable tunning search results

Ranking	W_l	**Alternate?**	δ_t	**c**	**NPV**	**Economic Limit (months)**	**Total Investment**	**FOPT (bbl)**	**FGPT (scf)**	**FWPT (bbl)**	**FWIT (bbl)**
1	50	1	12	1	$ 17,287,311.88	74	$ (29,000,000.00)	479.58E+3	406.45E-3	720.36E+3	1.20E+6
2	90	0	3	2	$ 16,086,695.70	58	$ (29,000,000.00)	433.46E+3	687.87E-3	338.81E+3	772.43E+3
3	90	0	1	2	$ 15,813,034.30	67	$ (29,000,000.00)	430.79E+3	1.79E+0	344.97E+3	775.90E+3
4	80	0	3	3	$ 15,660,571.71	35	$ (29,000,000.00)	410.33E+3	597.09E-3	141.63E+3	552.10E+3
5	90	0	6	2	$ 15,388,781.85	40	$ (29,000,000.00)	417.39E+3	434.92E-3	231.15E+3	648.69E+3
6	90	0	1	3	$ 15,258,942.03	41	$ (29,000,000.00)	434.95E+3	1.90E+0	366.77E+3	801.82E+3
7	50	1	1	1	$ 15,211,148.11	47	$ (29,000,000.00)	491.21E+3	2.32E+0	1.48E+6	1.97E+6
8	50	1	3	4	$ 15,152,740.78	50	$ (29,000,000.00)	472.12E+3	968.27E-3	852.59E+3	1.32E+6
9	50	1	1	3	$ 15,097,257.53	49	$ (29,000,000.00)	485.95E+3	2.39E+0	1.23E+6	1.72E+6
10	90	0	6	3	$ 15,072,423.34	42	$ (29,000,000.00)	424.96E+3	469.99E-3	301.54E+3	726.65E+3
11	50	1	3	1	$ 15,056,133.97	50	$ (29,000,000.00)	492.53E+3	937.01E-3	1.44E+6	1.93E+6
12	80	0	6	4	$ 15,035,316.73	41	$ (29,000,000.00)	416.62E+3	448.91E-3	228.03E+3	644.79E+3
13	80	0	1	4	$ 14,867,268.83	33	$ (29,000,000.00)	400.30E+3	1.15E+0	116.28E+3	516.77E+3
14	80	1	12	3	$ 14,863,433.15	51	$ (29,000,000.00)	488.06E+3	456.87E-3	1.28E+6	1.77E+6

6.2.4 Optimal Control

The nonlinear conjugate gradient algorithm was applied to this case as well in order to try to find the best possible solution. As pointed out before, there is the problem of the initial guesses, and the same methodology of the simple case was adopted here. For the sake of completeness, we are repeating the work flow as follows:

- 1 - The valves setting parameter found by the variable control.
- 2 - All valves opened since the beginning
- 3 - All valves set in mid range position since the beginning.

Since the simulation runs for 10 years and there is 6 ICVs in total, the vector u has 720 unknowns (120×6), which represents all valves set positions for the whole simulation time. This great number of variables supports use of the adjoint formulation to compute the gradient. The results of the algorithm are shown in table 6.16:

Table 6.16: Egg model - optimization results

Initial Guess	**NPV**	**Economic Limit (months)**	**FOPT (bbl)**	**FGPT (scf)**	**FWPT (bbl)**	**FWIT (bbl)**
1	$ 17,460,660.10	47	444.20E+3	590.04E-3	313.55E+3	757.91E+3
2	$ 13,184,990.03	45	426.27E+3	32.82E-3	444.40E+3	870.68E+3
3	$ 13,185,020.49	45	426.27E+3	32.79E-3	444.40E+3	870.68E+3

The optimal case, with the first type of initial guess, has a NPV very close to the variable control indicating a probable local solution.

6.2.5 Summary of Results

Table 6.17 summarizes the results found. The relative gains for this case are much bigger when compared to the simple case (relatives gains in the order of two digits).

Table 6.17: Egg model - summary

Case	**NPV**	**ΔNPV**	**ΔNPV%**
No ICV	$14.471E+06	$ -	0.00%
Optimal completions	$18.299E+06	**$3.828E+06**	**26.45%**
Variable Control	$17.287E+06	**$2.816E+06**	**15.39%**
Optimal Adjoint Method	$17.461E+06	**$2.989E+06**	**17.29%**

Figure 6.10 is the graphical representation of the results in table 6.17. The "optimal completions" scenario presents the best NPV gain amongst all scenarios, manly because of it lower initial capital expenditures (minus $1.8 million). However, such optimal completions configuration is unlikely to happen in real-world applications, since barely all completions should remain closed the whole time (table 6.14). Actually, if the reservoir model was fully characterized with 100% certainty, well 2 should not be drilled at all in the first place.

6.2.6 Robustness Check

It is clear though that the huge gains obtained in this case study (table 6.17) relies in a false assumption: total knowledge of the reservoir model. This is specially true for the scenarios "optimal completions" and "optimal control", where the configuration is defined *a priori*; while in the "variable control" scenario, the ICVs settings are defined in a reactive response to the water cut.

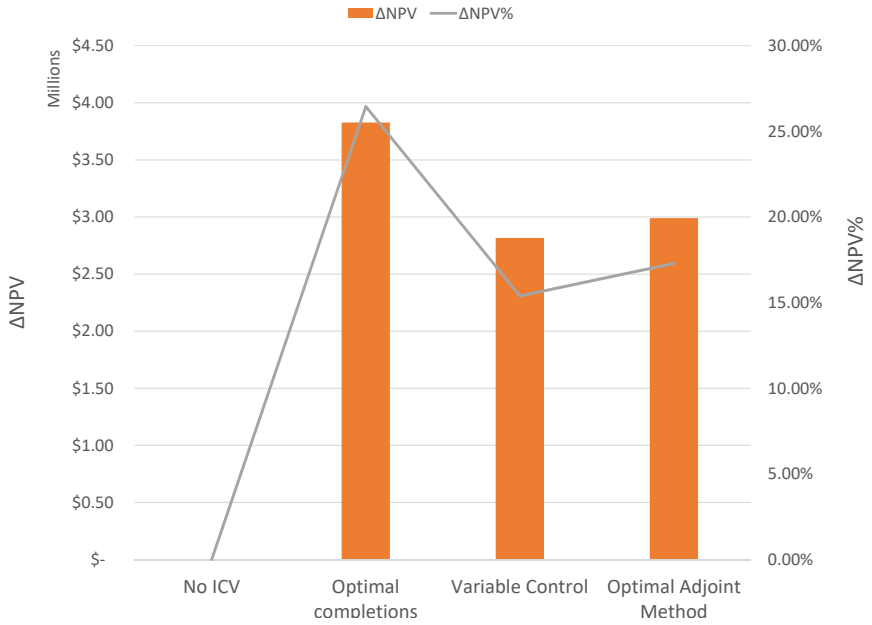

Figure 6.10: Egg model - summary

To deal with the geological uncertainties, this benchmark comes with more 100 realizations that, ideally, should account for every reservoir behavior. So, to check the robustness, all three strategies are ran over these realizations. But, in contrast from the previous sections, neither a tunning nor an optimization algorithm has been performed. In other words, the four tunning parameters (section 5.4.1) found in table 6.15 have been used, and the valves opening set configuration found from the optimizer algorithm in section 6.2.4 were implemented.

The box-plot is a convenient way to show all simulations in only one plot. So, fig. 6.11 shows the combination of four box plots: “fully open”, conventional wells completed in all layers; “best completions”, the best completion found in the base case scenario used in the other realization; “variable control”, the algorithm from section 5.4 with the previous tunned parameters; and the “optimal control”, the “a

priori" optimized valves settings configuration. In addition, the first slot has the value of the base case from the most probable realization, put here for comparison purposes.

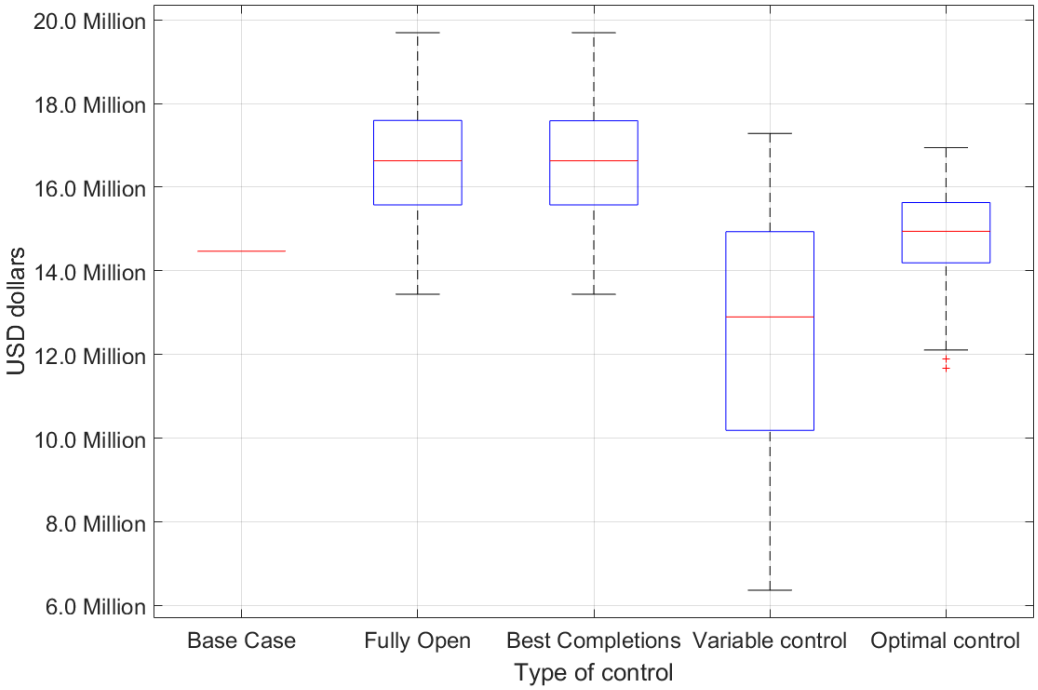

Figure 6.11: Box-plots distribution of the robustnesses check

Some conclusion can be taken from this plot.

- With the assumption that 101 realizations describe all possible reservoir dynamics, the most probable one proposed by the benchmark is actually a bad reservoir characterization, since its respective NPV below the first quartile.
- Although well 2 plays an important role in the base case, it seems to not interfere at all in the other realization. Since, the box plot for the "Best

completion" is almost the same than the "Fully open" plot. .

- The variable strategy based on watercut control has a large distribution (i.e. large standard deviation), and therefore it is a very risky strategy.
- In addition, the algorithm adopted for the variable strategy section 5.4 proved to be very depend on the tunning parameter. Comparing the "fully open" case with the base, there is a clear improvement in the NPV. On the other hand, the "variable control" had a tendency to decrease.
- Surprisingly, ad hoc "optimal control" seems to be safer than the variable control, but as expected, it showed worse results than the "Fully open case".

7. CONCLUSION

A simple smart logic for controlling inflow control valves in waterflooding reservoir management was implement and analyzed, with the final objective of improving the financial return of a petroleum reservoir in the long term, where the net-present-value was used as the measurement criteria. Three scenarios were constructed in order to make comparisons: one trial-and error to identify the best completion configuration, one variable control that uses the simple logic and an optimal solution, used as benchmark, found by commercial optimization algorithms. Finally, all strategies were tested in different realization to mimic the geologic uncertainties

Based on the work performed in this thesis, we can conclude:

- Simple controllers based on reactive logic under a water-cut loop can improve production strategies. Specially in complex reservoir with several wells and heterogeneous permeability field, the gain in relation to net-present value was considerable. On the other hand, in simple reservoir configurations and homogeneous permeability field, the differences are not so pronounced.

- Simple controllers achieved solutions close to gradient optimization algorithms. However, optimization problems are likely to be trapped in local solutions due to the high nonlinear characteristic and large scale of a reservoir simulator.

- Reservoir characterization remains a key aspect any attempt to improve production. Since optimization techniques deeply rely on models and even the simpler controllers are very sensitive to certain parameter that need to be tunned according to models. If the most probable model is wrong, very little can be achieve.

- The benefit of simple smart logic could be improved by a periodically "history matching" in order to re-tune its parameters

7.1 Future Works

- Further research should be done regarding ICV allocation in a well.
- Moving to High Performance Computing (HPC) makes more sense to overcome computational bottlenecks.
- Different control loop with simple smart logic besides water cut should be take in consideration. For instance, oil flow control instead of water cut control, where a more
- Economic uncertainties should be taken into consideration, by adopting a decision tree method but preferable a risk approach, with the risk of failures in an ICV is added to the decision process.

REFERENCES

Addiego-Guevara, E., M. D. Jackson, and M. A. Giddins. 2008. "Insurance Value of Intelligent Well Technology against Reservoir Uncertainty." In *SPE Improved Oil Recovery Symposium.* Society of Petroleum Engineers. doi:10.2118/113918-MS.

Adeyemo, K. M., C. Aigbe, I. C. Chukwumaeze, D. Meinert, and S. Shyrock. 2009. "Intelligent Well Completions in Agbami: A Review of the Value Added and Execution Performance." In *Offshore Technology Conference.* Offshore Technology Conference. doi:10.4043/20191-MS.

Ahmed, T. 2010. *Reservoir Engineering Handbook.* 4th ed. Oxford: Elsevier.

Akram, N., S. Hicking, P. Blythe, P. Kavanagh, P. Reijnen, and D. Mathieson. 2001. "Intelligent Well Technology in Mature Assets." In *Offshore Europe Conference.* Society of Petroleum Engineers. doi:10.2118/71822-MS.

Al-Khelaiwi, F. T., V. M. Birchenko, M. R. Konopczynski, and D. Davies. 2010. "Advanced Wells: A Comprehensive Approach to the Selection between Passive and Active Inflow-control Completions." *SPE Production & Operations* 25 (03): 305–326. doi:10.2118/132976-PA.

Babadagli, T. 2007. "Development of Mature Oil Fields – a Review." *Journal of Petroleum Science and Engineering* 57 (3–4): 221–246. doi:10.1016/j.petrol.2006.10.006.

Capolei, A., E. Suwartadi, B. Foss, and J. B. Jørgensen. 2015. "A Mean-Variance Objective for Robust Production Optimization in Uncertain Geological Scenarios." *Journal of Petroleum Science and Engineering* 125 (January 2015): 23–37. doi:10.1016/j.petrol.2014.11.015.

Chacon, A., J. B. McCutcheon, D. W. Schott, B. J. Arias, and J. M. Wedgwood. 2007. "Na Kika Field Experiences in the Use of Intelligent Well Technology to Improve Reservoir Management." In *International Petroleum Technology Conference.* International Petroleum Technology Conference. doi:10.2523/IPTC-11784-MS.

Chen, C., G. Li, and A. C. Reynolds. 2012. "Robust Constrained Optimization of Short-and Long-Term Net Present Value for Closed-loop Reservoir Management." *SPE Journal* 17 (03): 849–864. doi:10.2118/141314-PA.

Chen, Z., G. Huan, and Y. Ma. 2006. *Computational Methods for Multiphase Flows in Porous Media.* Philadelphia: Society for Industrial / Applied Mathematics.

Collins, J. R., and E. B. Neubauer. 2012. "The Agbami Intelligent Well: Examples of Active Reservoir Management." In *SPE International Production and operations Conference.* Society of Petroleum Engineers. doi:10.2118/156670-MS.

Dilib, F. A., and M. D. Jackson. 2013. "Closed-loop Feedback Control for Production Optimization of Intelligent Wells under Uncertainty." *SPE Production & Operations* 28 (04): 345–357. doi:10.2118/150096-PA.

Dilib, F. A., M. D. Jackson, A. Mojaddam Zadeh, R. Aasheim, K. Årland, A. J. Gyllensten, and S. M. Erlandsen. 2015. "Closed-loop Feedback Control in Intelligent Wells: Application to a Heterogeneous, Thin Oil-rim Reservoir in the North Sea." *SPE Reservoir Evaluation & Engineering* 18 (01): 69–83. doi:10.2118/159550-PA.

EIA. 2014. *International Energy Outlook 2014: World Petroleum and Other Liquid Fuels.* Washington, DC: U. S. Energy Information Administration.

———. 2016. "What Drives Crude Oil Prices?: An Analysis of 7 Factors That Influence Oil Markets, with Chart Data Updated Monthly and Quarterly." Accessed March 18, 2016. https://www.eia.gov/finance/markets/spot_prices.cfm.

Ertekin, T., J. H. Abou-Kassem, and G. R. King. 2001. *Basic Applied Reservoir Simulation.* SPE textbook series: v. 7. Richardson, Texas, USA: Society of Petroleum Engineers.

Evensen, G. 2009. *Data Assimilation: The Ensemble Kalman Filter.* 2nd ed. Chap. Estimation in an oil reservoir simulator, 263–272. Berlin: Springer Berlin Heidelberg. doi:10.1007/978-3-642-03711-5_17.

Foss, B. A., and J. P. Jensen. 2011. "Performance Analysis for Closed-loop Reservoir Management." *SPE Journal* 16 (01): 183–190. doi:10.2118/138891-PA.

Gao, C. H., R. T. Rajeswaran, and E. Y. Nakagawa. 2007. "A Literature Review on Smart-well Technology." In *SPE Production and Operations Symposium.* Society of Petroleum Engineers. doi:10.2118/106011-MS.

Güyagüler, B., A. T. Papadopoulos, and J. A. Philpot. 2010. "Feedback Controllers for the Simulation of Field Processes." *SPE Reservoir Evaluation & Engineering* 13 (01): 10–23. doi:10.2118/118969-PA.

Hirst, T. 2014. "These 6 countries Will Be Screwed If Oil Prices Keep Falling." Business Insider. Accessed March 18, 2016. http://www.businessinsider.com/these-6-countries-will-be-screwed-if-oil-prices-keep-falling-2014-10.

Hou, J., K. Zhou, X.-S. Zhang, X.-D. Kang, and H. Xie. 2015. "A Review of Closed-loop Reservoir Management." *Petroleum Science* 12 (1): 114–128. doi:10.1007/s12182-014-0005-6.

IEA. 2015. *World Energy Outlook 2015.* Paris: OECD Publishing. doi:10.1787/weo-2015-en.

Investopedia. 2011. "Understanding the Sharpe Ratio." Accessed April 7, 2016. http://www.investopedia.com/articles/07/sharpe_ratio.asp.

Jansen, J.-D. 2011. "Adjoint-based Optimization of Multi-phase Flow through Porous Media - a Review." *Computers & Fluids* 46 (1): 40–51. doi:10.1016/j.compfluid.2010.09.039.

Jansen, J.-D., O. H. Bosgra, and P. M. J. Van den Hof. 2008. "Model-based Control of Multiphase Flow in Subsurface Oil Reservoirs." *Journal of Process Control* 18 (9): 846–855. doi:10.1016/j.jprocont.2008.06.011.

Jansen, J.-D., D. Brouwer, S. G. Douma, P. Van den Hof, O. Bosgra, and A. Heemink. 2009. "Closed-loop Reservoir Management." In *SPE Reservoir Simulation Symposium.* Society of Petroleum Engineers. doi:10.2118/119098-MS.

Jansen, J.-D., R. M. Fonseca, S. Kahrobaei, M. M. Siraj, G. M. Van Essen, and P. M. J. Van den Hof. 2014. "The Egg Model – a Geological Ensemble for Reservoir Simulation." *Geoscience Data Journal* 1 (2): 192–195. doi:10.1002/gdj3.21.

Jones, G. A., and K. J. Warner. 2016. "The 21st Century Population-energy-climate Nexus." *Energy Policy* 93 (June 2016): 206–212. doi:10.1016/j.enpol.2016.02.044.

Mian, M. A. 2011. *Project Economics and Decision Analysis: Determinisitic Models.* Tulsa, Oklahoma: PennWell Corporation.

Mubarak, S. M., N. Dawood, and S. Salamy. 2009. "Lessons Learned from 100 Intelligent Wells Equipped with Multiple Downhole Valves." In *SPE Saudi Arabia Section Technical Symposium and Exhibition.* Society of Petroleum Engineers. doi:10.2118/126089-MS.

Nævdal, G., D. R. Brouwer, and J.-D. Jansen. 2006. "Waterflooding Using Closed-loop Control." *Computational Geosciences* 10 (1): 37–60. doi:10.1007/s10596-005-9010-6.

Nocedal, J., and S. Wright. 2006. *Numerical Optimization.* 2nd ed. New York City: Springer-Verlag. doi:10.1007/978-0-387-40065-5.

Odeh, A. S. 1982. "An Overview of Mathematical Modeling of the Behavior of Hydrocarbon Reservoirs." *SIAM Review* 24 (3): 263–273. doi:10.1137/1024062.

Pinto, M. A. S. 2013. "Assited Optimization Mehod for Comparison between Conventional and Inteligent Wells Considering Uncertainties." PhD diss., UNICAMP.

Pinto, M., M. Ghasemi, N. Sorek, E. Gildin, and D. Schiozer. 2015. "Hybrid Optimization for Closed-loop Reservoir Management." In *SPE Reservoir Simulation Symposium.* Society of Petroleum Engineers. doi:10.2118/173278-MS.

Rascouet, A. 2015. "Oil States Need Price Jump to Balance Budget: Opec Reality Check." Blomberg Business. Accessed March 18, 2016. http://www.bloomberg.com/news/articles/2015-11-30/oil-states-need-price-jump-to-balance-budget-opec-reality-check.

Rodrigues, J. R. P. 2006. "Calculating Derivatives for Automatic History Matching." *Computational Geosciences* 10 (1): 119–136. doi:10.1007/s10596-005-9013-3.

Saputelli, L., M. Nikolaou, and M. J. Economides. 2005. "Self-learning Reservoir Management." *SPE Reservoir Evaluation & Engineering* 8 (06): 534–547. doi:10.2118/84064-PA.

———. 2006. "Real-time Reservoir Management: A Multiscale Adaptive Optimization and Control Approach." *Computational Geosciences* 10 (1): 61–96. doi:10.1007/s10596-005-9011-5.

Sarma, P., L. J. Durlofsky, K. Aziz, and W. H. Chen. 2006. "Efficient Real-time Reservoir Management Using Adjoint-based Optimal Control and Model Updating." *Computational Geosciences* 10 (1): 3–36. doi:10.1007/s10596-005-9009-z.

Satter, A., J. Varnon, and M. Hoang. 1994. "Integrated Reservoir Management." *Journal of Petroleum Technology* 46 (12): 1057–1064. doi:10.2118/22350-PA.

Schlumberger. 2014a. *Eclipse Reference Manual.* Version 2014.2. Schlumberger.

———. 2014b. *Eclipse Technical Description.* Version 2014.2. Schlumberger.

Thakur, G. C. 1996. "What Is Reservoir Management?" *Journal of Petroleum Technology* 48 (06): 520–525. doi:10.2118/26289-JPT.

The Economist. 2016. "Who's Afraid of Cheap Oil?: Low Energy Prices Ought to Be a Shot in the Arm for the Economy. Think Again." Accessed March 18, 2016. http://www.economist.com/news/leaders/21688854-low-energy-prices-ought-be-shot-arm-economy-think-again-whos-afraid-cheap.

The MathWorks Inc. 2015. *Matlab Version 8.5.0.* Natick, Massachusetts.

Towler, B. F. 2002. *Fundamental Principles of Reservoir Engineering.* SPE textbook series: v. 8. Richardson, Texas, USA: Henry L. Doherty Memorial Fund of AIME, Society of Petroleum Engineers, 2002.

Van Essen, G., P. Van den Hof, and J.-D. Jansen. 2011. "Hierarchical Long-term and Short-term Production Optimization." *SPE Journal* 16 (01): 191–199. doi:10.2118/124332-PA.

Van Essen, G., M. Zandvliet, P. Van den Hof, O. Bosgra, and J.-D. Jansen. 2009. "Robust Waterflooding Optimization of Multiple Geological Scenarios." *SPE Journal* 14 (01): 202–210. doi:10.2118/102913-PA.

Warner Jr., H. 2015. *Reservoir Engineering Aspects of Waterflooding.* 2nd ed. Richardson, Texas, USA: Society of Petroleum Engineers.

Wiggins, M., and R. Startzman. 1990. "An Approach to Reservoir Management." In *SPE Annual Technical Conference and Exhibition.* Society of Petroleum Engineers. doi:10.2118/20747-MS.

Zhou, F., X. Hu, and J. Liu. 2015. "Comparative Study of Feedback Control Policies in Water Flooding Production." *Journal of Natural Gas Science and Engineering* 27 (3): 1348–1356. doi:10.1016/j.jngse.2015.09.020.